Advances in Water Resources 136 (2020) 103484

Contents lists available at ScienceDirect

Advances in Water Resources

journal homepage: www.elsevier.com/locate/advwatres

Updating urban design floods for changes in central tendency and variability using regression

Jory S. Hecht*, Richard M. Vogel

Department of Civil and Environmental Engineering, Tufts University, Medford, MA 02155, USA

ARTICLE INFO

Keywords:
Flood frequency analysis
Heteroscedasticity
Nonstationarity
Regression
Urbanization
Variability

ABSTRACT

Ordinary least squares (OLS) regression offers a decision-oriented approach for modeling trends in annual peak flows. We introduce a two-stage OLS approach for nonstationary flood frequency analysis that (i) models changes in their central tendency (median) in response to environmental perturbations with one regression and then (ii) examines changes in the coefficient of variation (Cv) by running a second regression on Anscombe-transformed residuals from the first regression. Monte Carlo simulations show that this approach yields 100-year flood estimates with mean squared errors comparable to estimates made with an advanced generalized linear model-based method. Also, this second-stage regression often produces approximately normal residuals, which permits statistical inferences on Cv trends. Case studies illustrate the dramatic impact that decreasing and increasing Cv trends can have on 100-year floods. Findings motivate the incorporation of trends in variability in infrastructure design along with further research examining asymmetric changes in urban flood variability.

1. Introduction

Worldwide, floods cause an estimated $24 billion damage and the loss of thousands of lives annually (Kundzewicz et al., 2014). Observed and anticipated increases in flooding have spawned many new statistical methods for modeling changes in flood probability distributions over time (e.g. Strupczewski et al., 2001; Khaliq et al., 2006; Vogel et al., 2011; Salas et al., 2018) and in response to specific environmental perturbations, such as climate change (e.g. Jain and Lall, 2000; Kwon et al., 2008; Condon et al., 2015), urbanization (e.g. Beighley and Moglen, 2003; Villarini et al., 2009b; Gilroy and McCuen, 2012; Prosdocimi et al., 2015; Over et al., 2016; Oudin et al., 2018) and reservoir storage (e.g. López and Francés, 2013; Over et al., 2016). This includes numerous approaches that address the following question: "What is the magnitude of a flood expected once every 100 years (or another recurrence interval of interest) on average given *current conditions* in a basin?" While planners increasingly seek tools to characterize these changes, many national-level agencies are still working to establish design guidelines to reflect them. For instance, the United States' Bulletin 17C notes that practices for adjusting design floods for changes in basin conditions require more research before specific recommendations can be made (England et al., 2018, p. 23). National institutions have recommended numerous safety factors, statistical methods and mechanistic models for adjusting design flood estimates for ongoing anthropogenic perturbations (Kjeldsen et al., 2008; Madsen et al., 2013; Prosdocimi et al., 2014; ASFPM, 2016 (recently rescinded, see FEMA and DHS, 2018); Ball et al., 2016), but few best practices have been established. Moreover, some fundamental questions regarding changes in flood regimes, such as changes in urban flood variability, require more research before standard methods are instituted.

Many flood frequency analyses (FFA) that account for ongoing changes in basin conditions have been criticized for improperly distinguishing between deterministic and stochastic components of change (e.g. Montanari and Koutsoyiannis, 2014; Serinaldi et al., 2018). True changes in probability distributions of stochastic phenomena, such as precipitation, are more difficult to diagnose in small samples typical of hydroclimatic records since they may be conflated with long-term persistence and other forms of natural variability (e.g. Cohn and Lins, 2005; Luke et al., 2016). However, unequivocal deterministic changes in phenomena that are not subject to sampling uncertainty stemming from interannual fluctuations can also affect flood probability distributions. In fact, prior reviews have found that most annual maximum series (AMS) of instantaneous peak flows which exhibit strong evidence of nonstationarity are associated with major deterministic basin changes, such as urbanization (e.g. Villarini et al., 2009a; Villarini and Smith, 2010). This makes methods for adjusting FFA in basins that have undergone such deterministic changes especially compelling (e.g. Serinaldi and Kilsby, 2015).

Changes in variability are a fundamental aspect of nonstationary FFA (NSFFA) that is increasingly receiving attention (e.g. Strupczewski et al., 2001; Cunderlik and Burn, 2003; Villarini et al., 2009a; Delgado et al., 2010; Delgado et al., 2014; O'Brien and Burn, 2014; Condon et al.,

* Corresponding author at: U.S. Geological Survey, Reston, VA 20192, USA
E-mail address: jhecht@usgs.gov (J.S. Hecht).

https://doi.org/10.1016/j.advwatres.2019.103484
Received 24 March 2019; Received in revised form 20 October 2019; Accepted 3 December 2019
Available online 5 December 2019
0309-1708/Published by Elsevier Ltd.

2015; Ahn and Palmer, 2015; Spence and Brown, 2016; Yu and Stedinger, 2018). This is especially critical given the greater sensitivity of extreme design floods to trends in variability than to commensurate trends in central tendency (Katz and Brown, 1992). Yet, methods for adjusting probability distributions for deterministic changes in variability stemming from urbanization and other deterministic phenomena are still not as developed as those for trends in central tendency. Urbanization can decrease annual flood variability, as increases in impervious cover have been associated with greater increases in smaller floods than larger ones (e.g. Hollis, 1975; USACE, 1993; McCuen, 2003; Kjeldsen, 2010; Braud et al., 2013; Over et al., 2016). In contrast, cross-sectional studies associating greater drainage densities with greater annual flood variability (Pallard et al., 2009) suggest that urbanization-induced increases in drainage density may also amplify flood variability, though this has not been assessed in urban areas with confined subsurface drainage networks (Ogden et al., 2011). Changes in precipitation have also failed to explain other observed increases in urban flood variability (Villarini et al., 2009; Trudeau and Richardson, 2016).

Practical approaches for characterizing changes in both the central tendency and variability of floods must address decision-makers and stakeholder concerns. Hecht (2017) and Serago and Vogel (2018) outline many benefits of regression for NSFFA, which, taken together, offer numerous features well suited for decision-oriented analyses. First, its ease of use, effective graphical communication, and parsimonious estimation of conditional moments makes it an attractive alternative to many advanced methods. (See Serago and Vogel (2018) for more on the value of parsimonious models in FFA.) Second, regression offers decision-relevant information, including expressions of uncertainty (confidence and prediction intervals) and enables hypothesis tests regarding the influence of covariates on changing floods (e.g. Kwon et al. 2008; Prosdocimi et al. 2014). Such tests are valid when model residuals are serially uncorrelated, normally distributed and homoscedastic (constant variance), or when standard error distortions from heteroscedastic (non-constant variance) residuals can be sufficiently ameliorated using heteroscedasticity-consistent standard errors (e.g. Long and Ervin, 2000) or through weighted or generalized least-squares regression (Stedinger and Tasker, 1985; Kjeldsen and Jones, 2009). Regression also accommodates many smooth nonlinear functions through “ladders of powers” transformations (Mosteller and Tukey, 1977) as well as abrupt changes (Bates et al., 2012), missing data (Slater and Villarini, 2016), and analytical corrections to the variance of regression coefficients inflated by short- and long-term persistence (Matalas and Sankarasubramanian, 2003). Prior applications also demonstrate its suitability for NSFFA.

While curtailing heteroscedasticity to minimize standard error distortions is critical for many statistical applications, the non-constant variance of residuals also provides valuable information about a phenomenon’s variability, especially when associated with physical covariates. One can use regression to model trends in variability by first modeling changes in central tendency using one regression, and then fitting a second-stage regression on the transformed squared residuals from the first-stage regression (Carroll and Ruppert, 1988). As we show later, transforming squared first-stage residuals can produce second-stage residuals well approximated by a normal distribution, which enables statistical inferences on variability trends. This two-stage regression approach, known variously as heteroscedastic regression (e.g. Smyth et al., 2001; Zheng et al., 2013), variance function regression (e.g. Davidian and Carroll, 1987), or parametric dual modeling (Robinson and Birch, 2000), has been used for over half a century (Park, 1966; Harvey, 1976). As Western and Bloome (2009) note, it has been employed in diverse disciplines, including for pharmacological dose-response curves (e.g. Davidian and Haaland, 1990), fish survival rates (Minto et al., 2008), housing prices (Zhang et al., 2015), climate change impacts to crop yields (Kelbore, 2012), ex-prisoner income (Western and Bloome, 2009), as well as many industrial applications (Smyth et al., 2001).

While other studies have modeled heteroscedasticity in continuous hydrologic time series (e.g. Wang, 2005; Sun et al., 2017; Fathian et al., 2019), few have used it to assess flood regimes. Latraverse et al. (2002) used a nonparametric form of local polynomial regression robust to heteroscedasticity for regional quantile estimates and Lim (2016) examined it when characterizing the variable source areas of urban flooding. Yet, the gap in practical methods for adjusting design events for changes in variability that McCuen (2003) identified has lingered. Despite the benefits of OLS regression, few studies have examined its ability to model changes in the coefficient of variation (Cv) and incorporate them into design flood estimates. Recently, Yu and Stedinger (2018) applied a two-stage regression approach to estimate trends in AMS variability, but their work differs from ours in three respects. First, when estimating changes in variability, they used nonlinear least-absolute value regression instead of OLS regression, the latter with which stakeholders and decision makers are likely to be more familiar. Second, we also compare our OLS-based method to a more advanced approach combining iteratively weighted least squares and generalized linear models (GLMs) (Aitkin, 1987). Third, we evaluate the feasibility of this model for urbanizing basins and parameterize our Monte Carlo experiment based on observed changes in annual peak flows in urbanizing basins.

To demonstrate our approach, we consider 100-year flood estimates made using the AMS of instantaneous peak flows in urbanizing basins in the United States. (See Stedinger et al. (1993, section 18.6.1) and Stedinger (2016, Section 76.2.3) and associated references for further guidance on when an AMS analysis is preferred over a POT one.) We use Total Impervious Area (TIA) as an example of a physical covariate which exhibits an unequivocal deterministic change over time. However, our approach can explore relationships between any covariate (e.g. climate indices) and annual floods. In addition, it can be extended to accommodate multiple covariates, including different ones in the first- and second-stage models.

This paper is organized as follows. Section 2 introduces regression-based methods for adjusting design flood estimates for trends in both the mean and variance of the natural logarithms of AMS, which are monotonically related to real-space trends in the median and Cv, respectively. Section 3 presents a Monte Carlo simulation experiment that compares the performance of four design flood adjustment methods. Section 4 provides case study illustrations and examines single-site trends in the median and Cv of AMS in urbanizing basins in the United States. Section 5 discusses limitations and possible extensions pertaining to both model development and planning applications, while Section 6 concludes.

2. Methods

2.1. Model overview

In FFA, one typically uses maximum likelihood, L-moments or the method of moments to estimate the parameters of a probability distribution. Here, we use the method of moments, where the unconditional moments of the natural logarithms of the AMS are replaced by their values conditioned upon physical covariates, i.e. explanatory variables, to reflect deterministic changes to a basin’s flood response. We introduce our approach using bivariate regression equations with the log-transformed AMS as the response variable and total impervious area (TIA) as the lone covariate (see Section 3). However, it can be extended to multivariate models.

While heteroscedastic regression can accommodate AMS approximating many distribution types (see Serago and Vogel, 2018), we introduce our two-stage regression approach for AMS that arise from a two-parameter lognormal (LN2) distribution. This distribution often approximates AMS well under both stationary (Beard et al., 1974; Stedinger, 1980; Vogel and Wilson, 1996) and nonstationary conditions (e.g. Strupczewski et al., 2001; Vogel et al., 2011; Delgado et al.,

Table 1
Models for adjusting design floods to represent the most recent year of record.

		Log-space trends		Real-space trends		
Abbrev.	Model Name	Mean (μ_y)	S.D. (σ_y)	Median (Med_Q)	Cv (Cv_Q)	Description
S-LN2	Stationary LN2					No regression models needed. AMS follows LN2 distribution with constant (covariate-invariant) parameters.
HOM-NS-LN2	Homoscedastic Nonstationary LN2	X	X	X		One regression model produces AMS with LN2 distribution with a covariate-conditional median.
HET-NS-LN2	Heteroscedastic Nonstationary LN2	X	X	X	X	Two regression models produce AMS with LN2 distribution with a covariate-conditional median and Cv.
IWLS-GLM	Iteratively weighted least-squares (IWLS-GLM)	X	X	X	X	Two regression models produce AMS with LN2 distribution with a covariate- conditional median and Cv.

2014; Prosdocimi et al., 2014). Under stationary conditions, this parsimonious distribution can produce lower mean squared errors (MSE) associated with quantile estimates than numerous three-parameter distributions often used in FFA (Kuczera, 1982). This distribution is also especially attractive for NSFFA because it requires just four estimated parameters when the mean and variance of log-transformed values change linearly with one covariate (Aissaoui-Fqayeh et al., 2009). Vogel et al. (2011) also demonstrate the promise of OLS regression for modeling time-conditional LN2 distributions, as this model yields residuals which are well approximated by a normal distribution for over 75% of 19,430 AMS at unregulated and regulated gauging records of at least ten years in the United States. However, we emphasize that this approach could be applied to other two- and three-parameter probability distribution functions (pdfs) often used in FFA, including the generalized extreme value (GEV) and log-Pearson type III (LP3) pdfs, provided the resulting regressions exhibit normally distributed and uncorrelated residuals (see Serago and Vogel, 2018).

Consider a logarithmic transformation of the AMS discharges Q:

$$Y = \ln(Q) \tag{1}$$

If Q follows a LN2 pdf, then Y is normally distributed. Here, we present a two-stage regression modeling procedure, which yields estimates of the mean and variance of Y conditioned on the value of a physical covariate exhibiting a deterministic change. We define the nonstationary flood quantile function of discharge Q with covariate-conditional moments as follows:

$$Q_{p|\omega} = \exp\left(\mu_{y|\omega} + z_p \sigma_{y|\omega}\right) \tag{2}$$

where $Q_{p|\omega}$ is the annual flood with non-exceedance probability p for a covariate value ω, $\mu_{y|\omega}$ and $\sigma_{y|\omega}$ are the conditional mean and standard deviation, respectively, of the logs of the AMS, and z_p is a standard normal variate. For an LN2 distribution, a trend in the log-space mean corresponds to a trend in the real-space median because the mean of logs is the 50th percentile (median) of the LN2 distribution. A trend in the log-space mean $\mu_{y|\omega}$ also implies a commensurate trend in the real-space variance, which, in turn, enables the real-space Cv to remain unchanged. Also, when there is no trend in the log-space variance, there is no trend in the real-space Cv either since $Cv_Q = \sqrt{\exp(\sigma_y^2) - 1}$. Thus, we henceforth refer to trends in the mean and variance of log-transformed AMS as trends in the median and Cv, respectively.

Next, we derive conditional moments of Y corresponding to AMS arising from an LN2 distribution as an example. First, we derive a nonstationary LN2 quantile function using a homoscedastic regression model with trends in the mean of the logs, but no error variance trend, i.e. the real-space Cv is constant. Then, we turn to a heteroscedastic model that considers temporal changes in the log-space error variance (real-space Cv) as well as the mean of the logs (real-space median). Finally, we compare quantile estimates from these derived models to ones from an iteratively weighted least square – generalized linear model (Aitkin, 1987). Table 1 summarizes these four models.

2.2. Homoscedastic nonstationary regression model (HOM-NS-LN2)

Numerous NSFFA studies, including Vogel et al. (2011), Prosdocimi et al. (2014), Read and Vogel (2015), Over et al. (2016), Yu and Stedinger, (2018) and Serago and Vogel (2018), have employed a linear regression of the natural logarithms of the AMS $Y = ln(Q)$ on an explanatory variable ω:

$$Y = \beta_0 + \beta_1 \omega + \varepsilon \tag{3}$$

where β_0 and β_1 are regression coefficients and ε is a normally distributed, zero-mean error term with a constant variance. Over et al. (2016) show that models with this functional form nicely characterize the response of AMS to linear increases in TIA in the Chicago metropolitan area. When the residuals ε in (3) are homoscedastic and normally distributed, further statistical inferences can be made on β_0 and β_1 along with the overall model. Since the expected value of the residuals is zero, the conditional expectation of Y is:

$$E[Y(\omega)] = \mu_{y|\omega_0} = \beta_0 + \beta_1 \omega_0 \tag{4}$$

where $\mu_{y|\omega_0}$ denotes that the mean of Y is conditioned upon a covariate of a given value ω_0.

In a regression model, trends in the conditional mean directly impact the error variance estimated with residuals and, consequently, they affect the conditional variance. One can partition the variance of a dependent variable Y into two components: one explained by a covariate trend and another one comprised of the unexplained variance:

$$\sigma_y^2 = \beta^2 \sigma_\omega^2 + \sigma_\varepsilon^2 \tag{5}$$

This equation is best understood by considering two extreme cases: (i) when a trend is perfectly explained by the regression (i.e. $\sigma_y^2 = \beta^2 \sigma_\omega^2$), all data fall exactly on the trend line and the residual variance disappears entirely, and (ii) when there is no trend, the variance in the dependent variable arises strictly from the error variance alone (i.e. $\sigma_y^2 = \sigma_\varepsilon^2$). Meanwhile, the variance of Y conditional upon a given covariate ω_0 is equal to the model error variance σ_ε^2 since β_0, β_1, and ω_0 are all constant:

$$Var\left(Y|\omega_0\right) = \sigma_{y|\omega_0}^2 = \sigma_\varepsilon^2 \tag{6}$$

Next, when errors are homoscedastic (constant), σ_ε^2 is:

$$\sigma_\varepsilon^2 = \sigma_y^2 - \beta_1^2 \sigma_\omega^2 \tag{7}$$

Importantly, when estimating σ_ε^2 from residuals of a bivariate regression, a degrees of freedom correction factor *n-2* produces an unbiased estimate of the error variance:

$$\hat{\sigma}_\varepsilon^2 = \frac{1}{(N-2)} \sum_{i=1}^{N} \left(y_i - \hat{y}_i\right)^2 \tag{8}$$

where N is the AMS length, while y_i and $\hat{y}_i$ are the observed and modeled annual peak flows, respectively. Thus, HOM-NS-LN2 quantiles conditioned on a single covariate ω_0 are estimated as follows:

$$Q_{p|\omega_0} = \exp\left(\mu_{y|\omega_0} + z_p \sigma_{y|\omega_0}\right) = \exp\left(\beta_0 + \beta_1 \omega_0 + z_p \sigma_\varepsilon\right) \tag{9}$$

Note that (7) can also be expressed in terms of the Pearson correlation coefficient $\rho_{\omega,y}$:

$$\sigma^2_{y|\omega} = \sigma^2_{\varepsilon} = \left(1 - \rho^2_{\omega,y}\right)\sigma^2_y \tag{10}$$

where $\rho_{\omega,y} = \beta_1 \frac{\sigma_\omega}{\sigma_y}$. Many prominent FFA studies (e.g. Stedinger and Griffis, 2011; Vogel et al., 2011; Prosdocimi et al. 2014; Luke et al., 2016) have not considered reductions in the conditional variance of Y proportional to $\rho^2_{\omega,y}$ given in (10). Read and Vogel (2015) also show that reductions in $\sigma^2_{y|\omega}$ also lower the conditional real-space Cv $Cv_{Q|\omega}$ as follows:

$$Cv_{Q|\omega} = \sqrt{\left(Cv_Q^2 + 1\right)^{\left(1-\rho_{\omega,y}{}^2\right)} - 1} \tag{11}$$

2.3. Heteroscedastic nonstationary regression model (HET-NS-LN2)

Next, heteroscedastic regression model residuals imply that the Cv of an AMS changes with physical covariate values. We derive a coupled, two-stage regression model for modeling heteroscedastic residuals (HET-NS-LN2) that ensures zero-mean residuals, preserves the sign of the residuals, and allows the Cv to vary with a covariate (see Appendix A). The parameters of this variance model can be estimated with a second OLS regression, which, in turn, yields residuals likely to follow an approximately normal distribution. We replace the covariate-independent error terms from (3) with covariate-dependent ones so that:

$$Y_\omega = \beta_0 + \beta_1\omega + \varepsilon_\omega = \beta_0 + \beta_1\omega + sign(\varepsilon_\omega)\left[\gamma_0 + \gamma_1\omega + \varphi_\omega\right]^{3/2} \tag{12}$$

where γ_0 and γ_1 are regression coefficients, and φ_ω is a normally distributed, zero-mean error term with a constant variance. This expression keeps the expected value of estimated residuals $\hat{\varepsilon}_\omega$ at zero and preserves their sign. As explained below, (12) also enables us to estimate the covariate-dependent error variance with a second-stage regression model that relates a covariate to the first-stage model errors in (3) raised to the two-thirds power, i.e. $\varepsilon_\omega^{2/3}$. While we illustrate this second-stage regression using the covariate ω from the first-stage model, different covariates may be used for each stage (e.g. an indicator of urbanization for changes in the median and a climate index, such as the North Atlantic Oscillation, for changes in the Cv).

Since (12) preserves the zero-mean property of ε_ω, the conditional mean $E[Y|\omega_0]$ is identical to the conditional mean of HOM-NS-LN2, i.e. $E[Y|\omega_0] = \mu_{y|\omega_0} = \beta_0 + \beta_1\omega_0$. Thus, $Var[\beta_0 + \beta_1\omega_0] = 0$, $Var(Y|\omega_0) = \sigma^2_{y|\omega_0} = \sigma^2_{\varepsilon|\omega_0}$. Next, since $E[\varepsilon^2_\omega] = \sigma^2_{\varepsilon|\omega}$, fitting an OLS regression with ${\varepsilon_\omega}^2$ as the response variable and ω as the explanatory variable may appear useful for estimating $\sigma^2_{y|\omega_0}$ and making inferences regarding the associated trend. However, if residuals from the first-stage regression are normally distributed, its squared residuals will follow a highly skewed χ^2 distribution. If these squared residuals are then used as the response variable in a second-stage regression, the second-stage residuals are unlikely to be normally distributed. In contrast, if we raise the first-stage residuals in (12) to the two-thirds power, we obtain a response variable that follows an approximately normal distribution, except at its lower tail (see Appendix B):

$$\varepsilon_\omega^{2/3} = \gamma_0 + \gamma_1\omega + \varphi_\omega \tag{13}$$

If this second-stage regression also yields normally distributed residuals, we can make statistical inferences on the second-stage model along with its coefficients γ_0 and γ_1. The transformation to the two-thirds power represents a simplified version of the Anscombe (1953) transformation, which converts variables arising from Gamma distributions - of which the χ^2 distribution is a special case - to approximately normal ones (Carroll and Ruppert, 1988). While this approach has been applied to transform Gamma-distributed wet-day precipitation data (e.g. Chandler and Wheater, 2002; Kigobe et al., 2011), we could not find any flood applications.

Ultimately, we want to use γ_0 and γ_1 to estimate $\sigma^2_{y|\omega_0}$. Since $\sigma^2_{y|\omega_0} = \sigma^2_{\varepsilon|\omega_0} = E[{\varepsilon_\omega}^2]$, it follows that:

$$\sigma^2_{y|\omega_0} = E\left[\left(\varepsilon_\omega^{2/3}\right)^3\right] = E\left[\left(\gamma_0 + \gamma_1\omega + \varphi_\omega\right)^3\right] \tag{14}$$

Importantly, one must include the error term ϕ_ω in (14) or else the estimate of $\sigma^2_{y|\omega_0}$ may be severely downward biased. This leads to the following expression for the conditional variance:

$$\sigma^2_{y|\omega_0} = \left(\gamma_0 + \gamma_1\omega_0\right)^3 + 3\sigma^2_\varphi\left(\gamma_0 + \gamma_1\omega_0\right) \tag{15}$$

The second term on the right-hand side of (15) is proportional to the error variance of the second-stage model σ^2_φ, which tends to comprise a large portion of the total variance of $\varepsilon^{2/3}$. In fact, R^2 values of the conditional Cv model range from just 0.06 to 0.24 at sites with Cv trends significant at the 95% level (see Section 3). In other words, σ^2_φ explains 76% to 94% of the variation in $\varepsilon^{2/3}$. Yet, even though Cv trends explain a small fraction of the overall interannual variability, neglecting this second term can cause estimates of extreme floods at sites with increasing median and Cv trends to be lower than estimates only considering median trends. When estimating σ^2_φ, the degrees-of-freedom correction factor in (8) should also be used.

Next, by substituting (15) into (9), we obtain the HET-NS-LN2 quantile function for adjusting design floods with a given annual nonexceedance probability p conditioned on a given covariate value ω_0 (see Appendix A for a full derivation):

$$\begin{aligned} Q_{p|\omega} &= \exp\left(\mu_{y|\omega_0} + z_p\sigma_{y|\omega_0}\right) \\ &= \exp\left[\beta_0 + \beta_1\omega_0 + z_p\sqrt{\left(\gamma_0 + \gamma_1\omega_0\right)^3 + 3\sigma^2_\varphi\left(\gamma_0 + \gamma_1\omega_0\right)}\right] \end{aligned} \tag{16}$$

2.4. An advanced two-stage approach with generalized linear models (IWLS-GLM)

We compared the HET-NS-LN2 model to a more sophisticated two-stage modeling approach using generalized linear models (GLMs). GLMs accommodate dependent variables with non-normal distributions belonging to the exponential family of distributions. Aitkin (1987) showed that using iteratively (re)weighted least squares (IWLS) estimation with variance estimates from Gamma GLMs with log link functions yields asymptotic maximum likelihood estimates. This prevents heteroscedasticity-induced errors in residual estimates from propagating to the Cv trend model. Although we assume a different variance change trajectory than Aitkin (1987), these benefits of IWLS-GLM also make it an attractive procedure for our approach. Despite these benefits, NSFFA studies have not used IWLS-GLM, as other prior studies using GLMs have either assessed changes in location parameters (Clarke, 2001; Clarke, 2002; Aissaoui-Fqayeh et al., 2006; Najibi and Devineni, 2018), or variability in the number of coastal nuisance floods (Vandenberg-Rodes et al., 2016).

The iterative IWLS-GLM approach is implemented as follows:

1. Fit the HOM-NS-LN2 model (assuming equal weights for just the first iteration)
2. Square residuals of the HOM-NS-LN2 model.
3. Fit a second-stage gamma GLM with a log link function using the glm2 package in R statistical software (R Core Team 2019).
4. Use reciprocals of fitted values of (3) as weights when fitting HOM-NS-LN2 in the next iteration. Repeat until convergence. (We did this ten times to ensure convergence to four decimal places.)

This method produces estimates of the conditional mean and variance that can subsequently be inserted into the conditional quantile function in (2) to compute the 100-year flood.

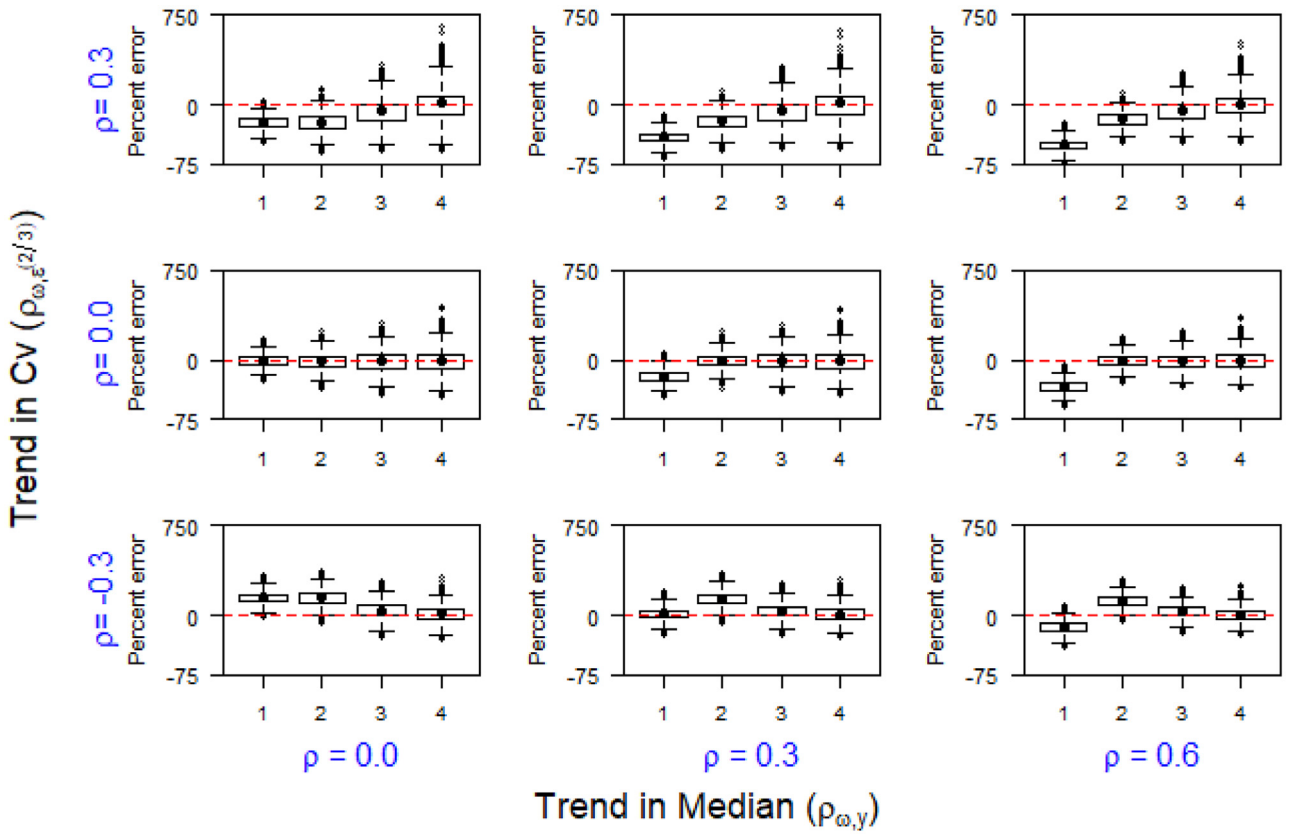

Fig. 1. Range of percent errors (percent bias) of 100-year flood estimates from simulated 50-year records sampled from LN2 annual flood distribution with Cv = 1 and various trends in the median and Cv for (1) S-LN2, (2) HOM-NS-LN2, (3) HET-NS-LN2, and (4) IWLS-GLM. Boxes show interquartile ranges of estimates, and the solid black points within them indicate the mean for each method. The whiskers extend from minimum values to 1.5 * interquartile range from the 75th percentile. Outliers above this upper bound are shown as points.

3. Monte Carlo simulation experiment

We conducted a Monte Carlo experiment to assess the accuracy of our design flood estimates for the last year of simulated 50-year records when using the four estimation methods listed in Table 1. We generated random samples of length 50 from a uniform distribution ranging from zero to one. Then, we treated these values as non-exceedance probabilities and computed annual flood values using covariate-conditional LN2 distributions with known initial parameters and change trajectories. We applied a three-factor experimental design in which we simulated 50-year AMS with different initial real-space Cv values, and different correlations driving their median and Cv trends ($\rho_{\omega,y}$, $\rho_{\omega,\varepsilon^{2/3}}$) based on our 202-station sample of urbanizing basins (see Section 4.3). We focused on cases with increases in the median and either increases or decreases in the Cv. Given planner interests in minimizing bias, uncertainty and worst-case outcomes, we computed the percent error distributions, percent bias (PBIAS), fractional root mean squared errors (fRMSE) and maximum possible over- and under-design errors of conditional quantile estimates for the last year of record from a set of 10,000 simulations. This experiment does not address general sampling issues that can cause downward biased estimates of the true 100-year flood value of a population (Stedinger, 1983). See Appendix D for more details on the experimental design and results.

The simulation experiments demonstrate that HET-NS-LN2 underpredicts the 100-year flood when there is an increasing Cv trend and overpredicts it when there is a decreasing one (Fig. 1). This transformation over-predicts lower-tail values and slightly underpredicts upper-tail ones (see Appendix B). As expected, design flood estimates considering modeling Cv trends (when present) are more accurate than ones that only consider trends in the median. The simulations of decreasing Cv trends also suggest that the S-LN2 quantile estimate may be better than HOM-NS-LN2 for modeling changes in extreme floods in urbanizing basins.

One pervasive question in nonstationary hydrology is whether the reduction in bias from adding model parameters is worthwhile given the increase in uncertainty that it can induce. For instance, Yu and Stedinger (2018) found that modeling changes in the Cv (log-space variance in their paper) only improves the RMSE under extreme changes. Yet, in this study, HET-NS-LN2 consistently registers a lower fRMSE than HOM-NS-LN2, which suggests that the bias reduction benefits of modeling Cv trends outweigh the increase in variance stemming from the addition of another parameter (Fig. 2). (See figures for other Cv values in Appendix D.)

We also compared HET-NS-LN2 and IWLS-GLM. As expected, IWLS-GLM estimates were considerably less biased. However, HET-NS-LN2 registers a lower fRMSE than IWLS-GLM, especially when the Cv is increasing. Also, maximum overdesign errors are larger under IWLS-GLM than HET-NS-LN2 when the Cv is increasing but slightly smaller when it is decreasing. In contrast, maximum under-design errors are slightly greater under IWLS-GLM regardless of the Cv trend direction. Thus, choices between these two methods depend on a decision maker's preference for unbiasedness versus minimizing uncertainty and worst-case outcomes. In addition, one could bias-correct HET-NS-LN2 results, as its bias is markedly correlated with the Cv (see Appendix D). However, we believe that other procedures for modeling Cv changes should be evaluated before attempting bias correction (see Section 5).

Finally, one must remember that this experiment only evaluates HET-NS-LN2 when simulated AMS originate from an LN2 distribution and the changes in moments follow the same trajectories that models assume. When the true Cv trend model followed the exponential

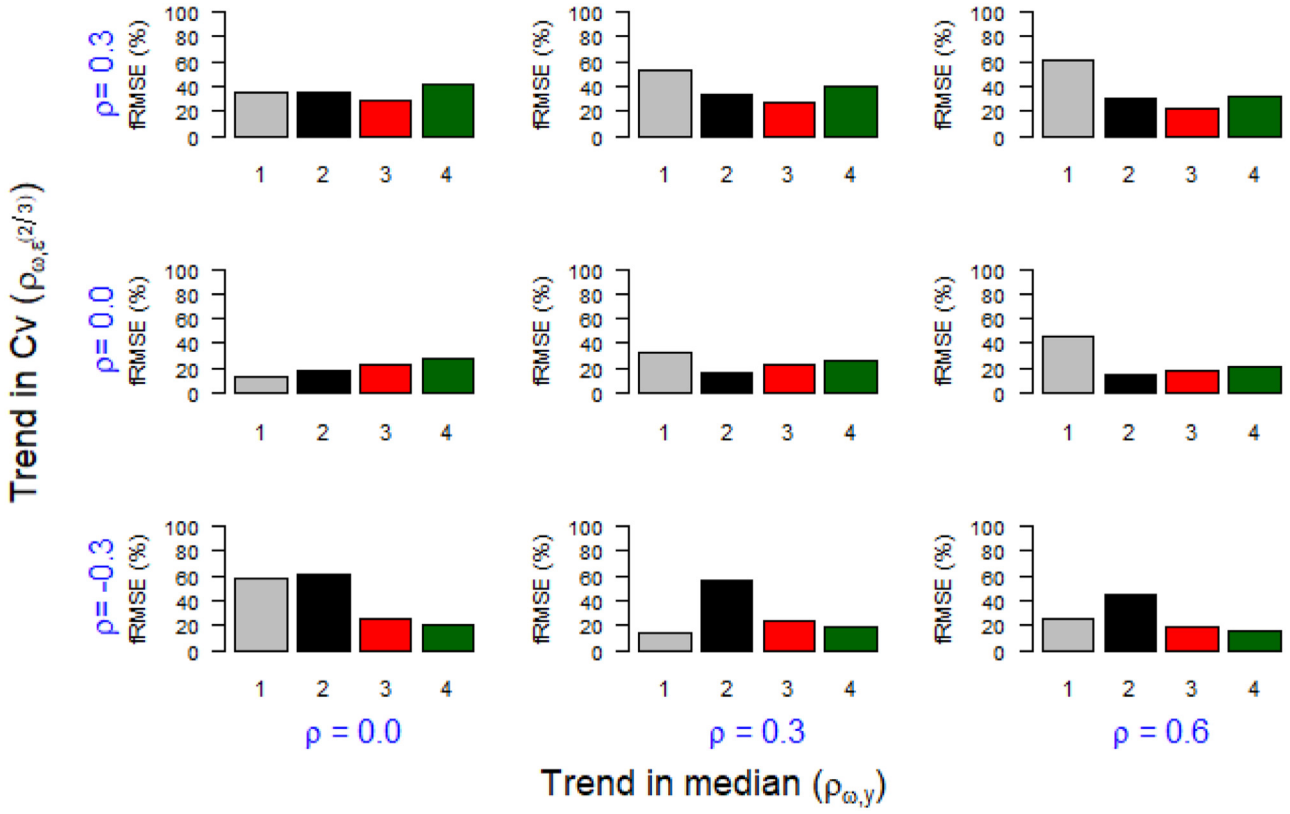

Fig. 2. Fractional root mean squared errors (fRMSE) of 100-year flood estimates from simulated 50-year records from (1) S-LN2, (2) HOM-NS-LN2, (3) HET-NS-LN2 and (4) IWLS-GLM. Simulated records sampled from LN2 annual flood distributions with Cv = 1 and various trends in the median and Cv indicated with correlation coefficients.

change trajectory that the Gamma GLM model assumes, HET-NS-LN2 still yielded lower fRMSE values than IWLS-GLM did for many trend combinations (see Appendix D). In practice, distribution types and change trajectories are unknown and prone to misspecification, which makes a more detailed robustness analyses examining the performance of our models when these assumptions are incorrect a natural sequitur to this study.

4. Applications

4.1. Urbanization effects on floods

Many aspects of urbanization alter flood regimes, leading to a wide range of responses (e.g. Smith et al., 2013; Salvadore et al., 2015; Zhou et al., 2017; Diem et al., 2018; Kokkonen et al., 2018). These urban drivers include increased impervious cover, soil compaction, stormwater routing and detention (e.g. Ogden et al., 2011; Miller et al., 2014), increased channel width and reduced overbank storage (Hirsch, 1977), return flows (Allaire et al., 2015; Oudin et al., 2018), groundwater pumping (Hopkins et al., 2015), induced recharge (Locatelli et al., 2017), and changes in precipitation due to urban heat islands (Yang et al., 2014). Underlying drivers of change, such as population growth, that lead to these hydrological impacts have also been identified (USACE, 1993; Villarini et al., 2009). Given these myriad flood-altering mechanisms, one major challenge with characterizing changes in urban flooding is the selection of indicators to represent urbanization. Standard approaches based on the percentage of total impervious area (TIA) have been criticized, especially in cross-sectional studies, because the relationship between TIA and flooding varies due to underlying soil types (Gregory et al., 2006), stormwater and drainage infrastructure (e.g. Leopold et al., 1968; Ogden et al., 2011; Miller et al., 2014; Zhou et al., 2017), the connectivity and spatial location of impervious cover (e.g. Mejia and Moglen, 2010; Ferreira et al., 2015; Debbage and Sheppard, 2018), as well as its diverse and time-variable hydrologic properties (Redfern et al., 2016), and mapped spatial resolution (Lee and Heaney, 2003; Weng, 2012). However, we argue that TIA is a suitable metric given our goal of demonstrating a method for adjusting design floods at individual sites where deterministic changes in the central tendency and variability of flooding are evident.

4.2. Illustrative case studies

We illustrate our NSFFA method with two case studies in small urbanizing basins, where prior studies have also documented urbanization-induced increases in flooding.

4.2.1. Increase in median, increase in Cv

The Aberjona basin in the Boston metropolitan area offers a natural laboratory for examining urbanization-induced changes in flooding (Allaire et al., 2015; Serago and Vogel, 2018; Villarini et al., 2018). The Aberjona River at Winchester station (Gage ID = 01102500, drainage area = 61.9 km^2) has recorded instantaneous peak flows since 1940. Here, TIA increases from 24.7% in 1940 to 37.7% in 2010. Fig. 3 demonstrates that trends in the median ($\rho_{\omega,y} = 0.46$, $p < 0.01$) and Cv ($\rho_{\omega,\varepsilon^{2/3}} = 0.29$, $p = 0.01$) exhibit highly significant positive correlations with TIA. It also shows that the stationary 100-year flood (44.9 m^3/s) roughly equals the flood of record (45.0 m^3/s). Under HOM-NS-LN2, the current 100-year flood rises to 53.0 m^3/s, an increase of 18%. Incorporating the Cv trend raises the 100-year flood to 64.9 m^3/s, which is 45% greater than the S-LN2 value. A Probability Plot Correlation Coefficient (PPCC) normality test fails to reject the null hypothesis that the residuals of the second-stage regression are normally distributed ($p = 0.39$). A modified Breusch-Pagan test (Breusch and Pagan, 1979), in which we regressed $\varepsilon^{2/3}$ on ω, also confirmed their homoscedasticity ($p = 0.86$).

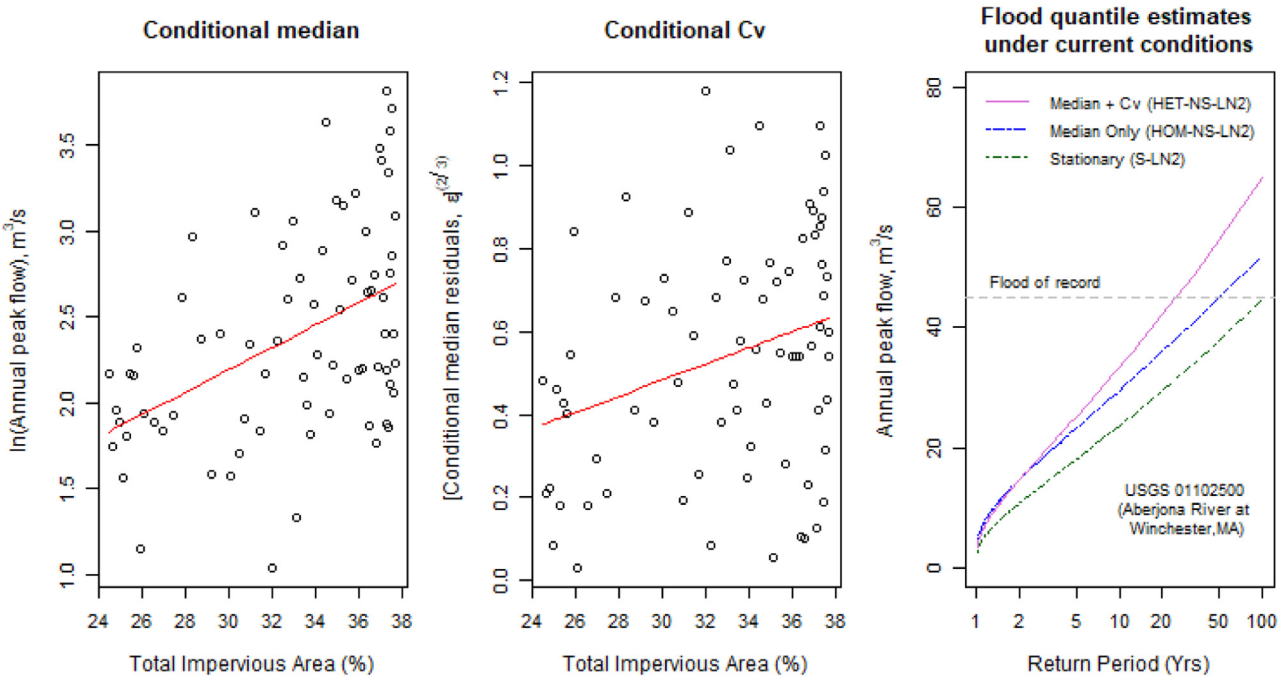

Fig. 3. Comparisons of nonstationary frequency curves for the Aberjona River at Winchester, Mass. (USGS 01102500) using: (a) conditional median regression (HOM-NS-LN2), (b) conditional Cv regression (HET-NS-LN2), and (c) quantile estimate comparison for floods with different frequencies under current (2016) conditions.

Together, these tests validate statistical inferences from the second-stage model. Recent increases in total and extreme precipitation (Ahn and Palmer, 2015; Huang et al., 2017), have not translated to increases in the Cv of annual floods in many less urbanized basins in eastern New England. Moreover, Hodgkins et al. (2017) find a lack of a contemporaneous increase in floods with recurrence intervals of 25–100 years in the northeastern United States. While further research is needed to untangle the effects of recent climatic fluctuations, including inter-decadal oscillations (see Armstrong et al., 2014; Berton et al., 2017) and an abrupt increase in extreme precipitation (Huang et al., 2017) from urban-induced changes in the Aberjona basin, the evidence presented strongly suggests that urbanization contributes to the increasing Cv here.

4.2.2. Increase in median, decrease in Cv

Fig. 4 shows that the AMS at the River Rouge at Birmingham, Michigan station (USGS ID 04166000, drainage area = 86.2 km^2), which has been operating since 1951, exhibits an increasing median and a decreasing Cv. The TIA of this basin, located in the western suburbs of the Detroit metropolitan area, steadily increased from 8.2% in 1950 to 24.7% in 2010. Fig. 4 exhibits a clear increase in the lower bound of the AMS while the upper bound has remained relatively constant. The lower bound continues to increase after 1970, a year when annual precipitation increased abruptly in the eastern U.S. (e.g. McCabe and Wolock, 2002). This provides another line of evidence that smaller annual floods have increased more than large ones. Aichele (2005) also detected an increase in maximum daily flows with a 1% exceedance probability between 1970 and 2003 at a 90% significance level and associated it with a 20% increase in residential area between 1980 and 2000. While Beam and Braunscheidel (1998) note that combined sewer overflows also contribute to peak runoff, there are no large flood-control reservoirs in the basin. A major drought from 1960–1967 (Paulson et al., 1991) may also enhance the median flood trend.

Overall, the increase in TIA exhibits a highly significant positive correlation ($\rho_{\omega,y} = 0.47$, $p < 0.01$) with the log-transformed annual floods while TIA has a highly significant negative correlation ($\rho_{\omega,\epsilon^{2/3}} = -0.37$, $p < 0.01$) with the Anscombe-transformed residuals. We could not reject the null hypotheses of normality and homoscedasticity of the second-stage residuals using a PPCC normality test ($p = 0.39$) and our modified Breusch-Pagan test for residual heteroscedasticity ($p = 0.21$), respectively. Importantly, accounting for the decreasing Cv trend in addition to the increasing median trend lowers the 100-year flood estimate by 28.8% - from 50.1 m^3/s with HOM-NS-LN2 to 35.7 m^3/s under HET-NS-LN2, which is even 13% lower than the S-LN2 estimate of 41.1 m^3/s.

However, Fig. 4 does not display strong visual evidence of a decrease in low-frequency events. A major reason for which the HET-NS-LN2 100-year flood is lower than its S-LN2 counterpart is that HET-NS-LN2 assumes a symmetric decrease in the variance of log-transformed annual peak flows, whereas numerous prior studies demonstrate a greater tendency for smaller floods to increase than for larger floods to decrease. A second reason is that the S-LN2 estimate may be upward biased because, when assuming stationarity, the site has a negatively skewed distribution (-0.59). While a nonstationary distribution fits quite well ($p = 0.59$), we must reject the stationary LN2 distribution of the AMS at this site using a PPCC normality test ($p < 0.01$). See Appendix C for a more detailed explanation. This discrepancy highlights problems with direct comparisons of stationary and non-stationary distributions, a challenge that motivated Serago and Vogel (2018) to create nonstationary probability plots to evaluate their goodness-of-fit.

4.3. Flood trends in urbanizing basins of the United States: a preliminary analysis

4.3.1. Identifying urbanizing basins with changing AMS

Numerous recent studies have analyzed floods in urbanizing basins throughout the United States (e.g. Salavati et al., 2016; Chao Lim, 2016; Luke et al., 2016; Oudin et al., 2018). We examined trends in the log-space mean (real-space median) and log-space variance (real-space Cv) in 202 urbanizing basins with at least 30 years of instantaneous peak flow observations through the 2016 water year (1 Oct – 30 Sep) and at least 10% impervious cover during one year in their station record. Please note that some stations with trends may have substantially different 100-year estimates using data beyond 2016, most notably stations in Houston due to major tropical cyclones in 2017 (see Zhang et al., 2018).

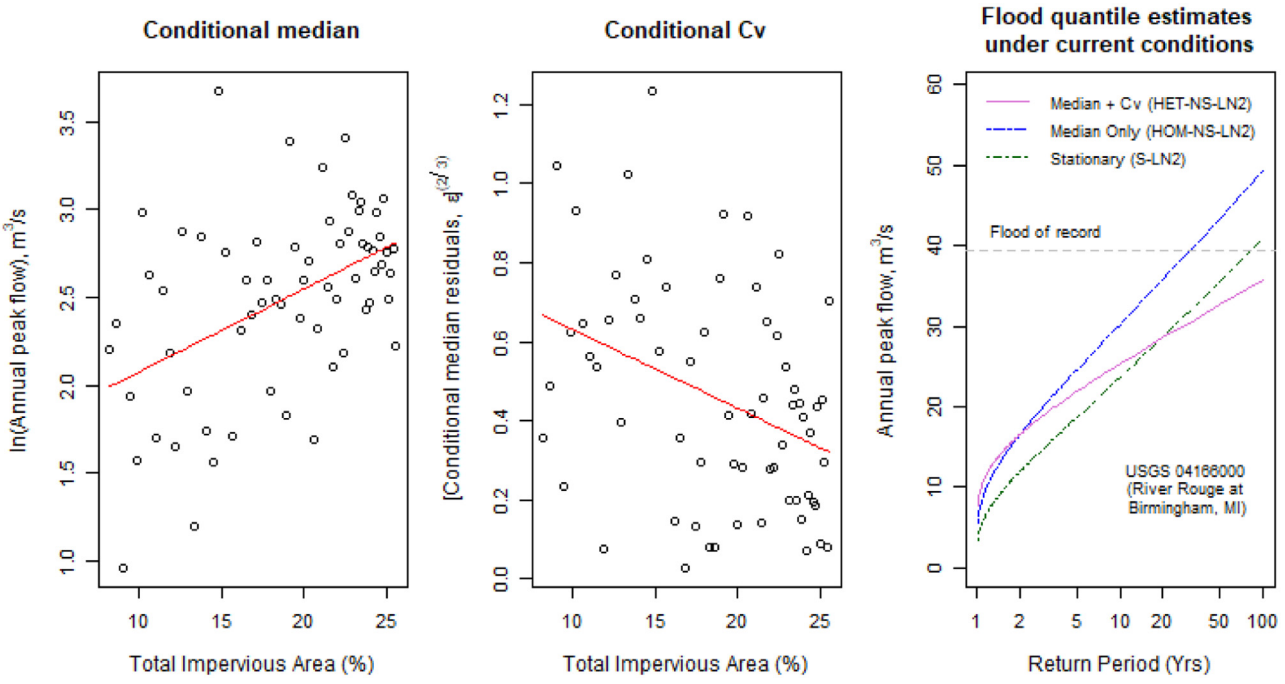

Fig. 4. Comparison of nonstationary frequency curves for the River Rouge at Birmingham, Mich. (USGS 04166000) using: (a) conditional median regression (HOM-NS-LN2), (b) conditional Cv regression (HET-NS-LN2), and (c) quantile estimate comparison for floods with different frequencies under current (2016) conditions.

Our study does not aim to identify an exhaustive subset of conterminous US basins with urbanization-altered floods or choose the best indicator of urbanization for attributing changes in design floods (e.g. Jato-Espino et al., 2018; Debbage and Shephard, 2018). Rather, we strive to examine the general prevalence of single-site Cv trends in urbanizing basins. Also, we are not aiming to draw any statistical conclusions about the prevalence of regional trends, which would require a spatial correlation analysis (Douglas et al., 2000).

Recent studies have used (i) basin attributes from the GAGES-II database (Falcone, 2011), including impervious cover thresholds (e.g. Oudin et al., 2018) and (ii) USGS Peak-Flow Qualification Codes (http://pubs.usgs.gov/wdr/2005/wdr-il-05/misc/peakcods.htm) (Luke et al., 2017) to identify urbanizing basins. We first removed individual annual instantaneous peak flow observations using Qualification Codes before removing entire station records based on their record lengths and other criteria. We eliminated peak flows with uncertain dates, maximum daily flows, dam failures and estimated historical floods. While historical floods during pre-instrumentation periods often provide valuable information, such records are more likely to exist for larger events than smaller ones. This could cause downward biases in estimates of trends in central tendency using OLS regression. Future research should evaluate the feasibility of integrating this method into FFA methods that accommodate historical records and other censored data, such as the Expected Moments Algorithm (Cohn et al., 1997).

Next, we used numerous criteria to select stations suitable for analysis. We removed all stations with AMS shorter than 30 years as Cunderlik and Burn (2003) recommended that AMS for testing trends in variability span at least 30-50 years to reduce the risk of confounding trends with inter-decadal variability. (Note that regression-based methods offer easily computable standard errors that allow for estimates of uncertainty that consider record lengths). To avoid misleading trend diagnoses when abnormally small or large annual floods lie at the beginning or end of an AMS (see Slater and Villarini, 2016), we also removed stations that had at least one 30-year period with fewer than ten annual peak flows. Stations with peak flows below 1 m^3/s were also omitted due to the challenges of gauging such low discharges combined with the pronounced effect that these low estimates could have on conditional median regression models fit in log-space. Changepoint tests in the mean and variance of the log-transformed AMS using the At Most One Change (AMOC) method in the *changepoints* package for R statistical software (R Core Team, 2019) did not reveal any AMS with changepoint confidence levels exceeding 95% when using minimum segment lengths of 10 years.

After performing this initial screening, we identified a subset of urbanizing basins. Following Oudin et al. (2018), we first applied the impervious cover fraction obtained from the widely used NLCD dataset to identify basins whose TIA exceeded 10% in 2006. While flood magnification has been detected in basins with less than 5% impervious cover (Yang et al., 2010) and depends upon underlying soils (e.g. Gregory, 2006), this standard threshold of 10% (Schueler, 2009) enabled us to identify a set of urbanizing basins suitable for demonstrating our modeling approach. We also only evaluated stations whose reservoir storage capacity was less than 10% of their mean annual flow according to GAGES-II. We then performed a more detailed analysis of changes in TIA from 1940–2016 using decadal housing density data (1940–2010) with a 1-km spatial resolution from Theobald (2005). We eliminated stations with drainage areas smaller than 5 km^2 due to the TIA data's coarse resolution. Each basin's TIA was computed using the reclassify and raster clipping functions in the Spatial Analyst extension of ArcGIS 10.4® (the same procedure can be implemented using freely available QGIS and GRASS-GIS software). We then applied previously validated relationships from Oudin et al. (2018) to estimate the TIA in each 1-km^2 cell based on housing density data and TIA on land used for commerce, industry and transportation. Decadal values were linearly interpolated to create annual time series for 202 urbanizing basins. TIA from 2010–2016 was assumed to increase at the same rate as during 2000–2010. Annual flood peaks prior to the beginning of TIA time series in 1940 were omitted from the analysis.

We then identified stations in this subset of 202 urbanizing basins that had AMS with first-stage (conditional median) residuals for which null hypotheses of normality and no lag-one correlation could not be rejected at a 95% significance level ($p \leq 0.05$). Using version 2.5 of the *sandwich* package in R, we computed all trend *p*-values using robust heteroscedasticity-consistent standard errors with the HC3 estimator,

Table 2
Number of AMS with signifcant ($p \leq 0.05$) trends in the real-space median and Cv in a sample of 135 urbanizing basins that have conditional median estimates with normally distributed and serially independent residuals. Numbers in parentheses indicate the percentage that each trend combination comprises in this 135-station sample.

+Cv	1 (0.7%)	3 (2.2%)	6 (4.4%)
0	1 (0.7%)	59 (43.7%)	53 (39.3%)
-Cv	1 (0.7%)	3 (2.2%)	8 (5.9%)
	− Med	0	+ Med

which adjusts squared residual values to correct for the effects of overly influential observations (Long and Ervin, 2000). We deemed all trends with $p \leq 0.05$ as "approximately statistically significant". At the 135 stations whose residuals were normally distributed and serially independent (67% of the 202 urban stations), we tested for trends in the Anscombe-transformed residuals using our modified Breusch-Pagan test.

4.3.2. Results

Table 2 shows the number of urbanizing basins from the 135-station sample with each of the nine possible combinations of trends in the conditional median (negative, insignificant, positive) and Cv (negative, insignificant, positive) using HET-NS-LN2. Fourteen of the 67 (21%) urbanizing basins with significant increases in their median annual flood also demonstrated significant concurrent changes in their Cv, with six sites exhibiting increasing Cv trends and eight sites (including one pair of nested sites in Houston, Texas) having decreasing trends. This suggests that HOM-NS-LN2 is valuable for modeling trends in many urbanizing basins with changing flood hazards, but it may neglect important changes to the relative variability of AMS in others. Differences between HET-NS-LN2 and IWLS-GLM estimates reflected ones obtained in the Monte Carlo experiments, as HET-NS-LN2 exhibited a greater upward (downward) bias than IWLS-GLM for decreasing (increasing) Cv trends (Appendix F). Fig. 5 maps stations with these different combinations of trends.

Observed Cv trends at stations with increasing median annual floods motivated us to apply HET-NS-LN2 in basins featuring both trends. While correlations between TIA and the Anscombe-transformed residuals of models with significant Cv trends are relatively weak, with ranges of 0.26 - 0.49 for increasing trends and 0.26 - 0.48 for decreasing trends, their pronounced effects on design floods make testing for Cv trends imperative. To further compare the models in Table 1, we calculated percent changes in nonstationary flood quantiles attributable to median and Cv trends. First, we computed the percent increase in the 100-year flood attributable only to increased medians $Q_{100yr}(\mu_{y|\omega})$:

$$\frac{Q_{100yr}(\mu_{y|\omega}) - Q_{100yr}}{Q_{100yr}} \tag{17}$$

where Q_{100yr} is the stationary (S-LN2) 100-year flood estimate. Next, we computed the difference between the estimate considering both median

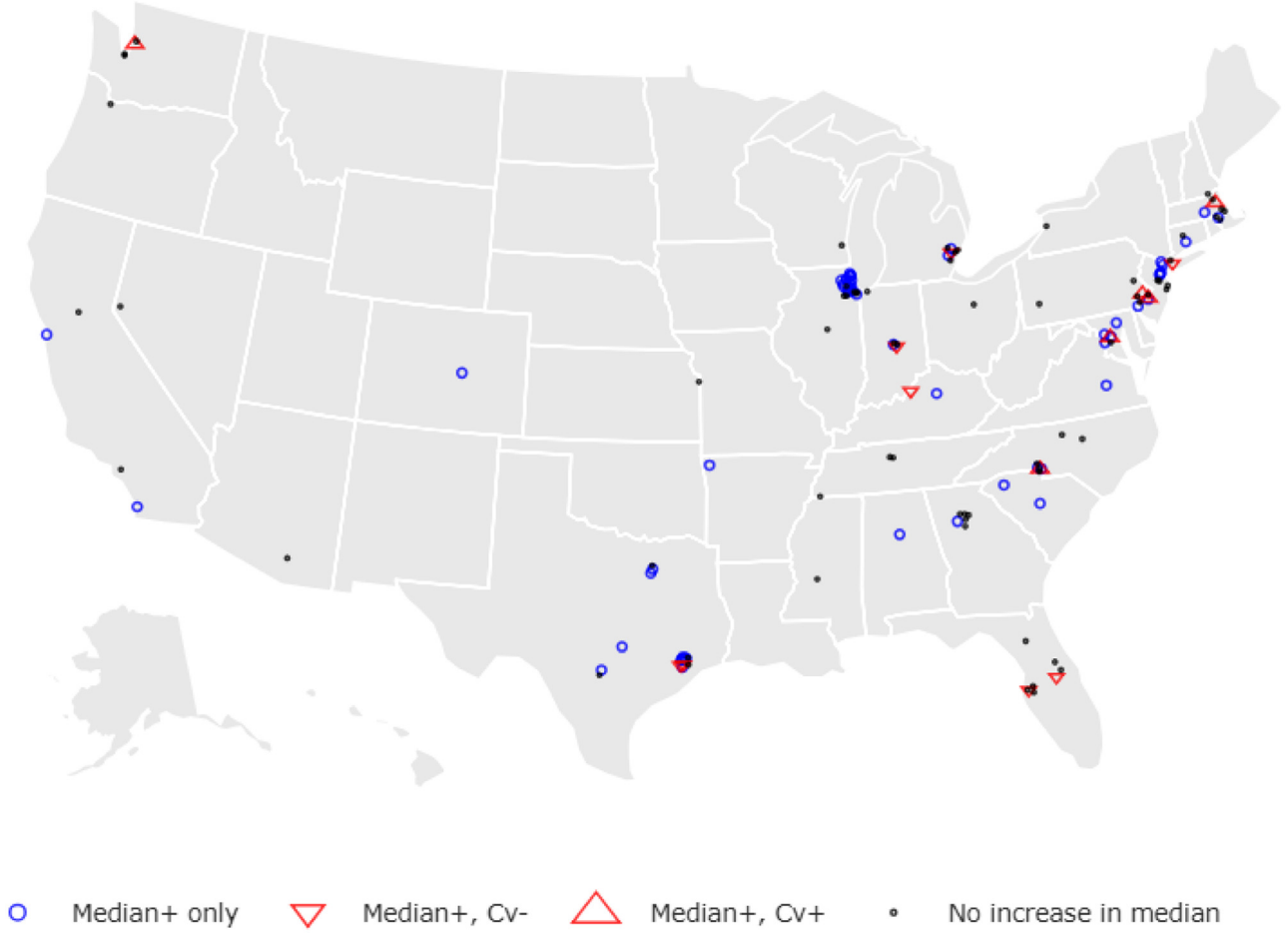

Fig. 5. Trends at 135 urbanizing basins analyzed in the United States with: (i) no increases in median annual flood (No increase), (ii) increasing median trends without any Cv trends (Median+ only), (iii) increasing median trends and decreasing Cv trends (Median+, Cv-), and (iv) increasing median and Cv trends (Median+, Cv+). All trends significant at 95% level ($p < 0.05$).

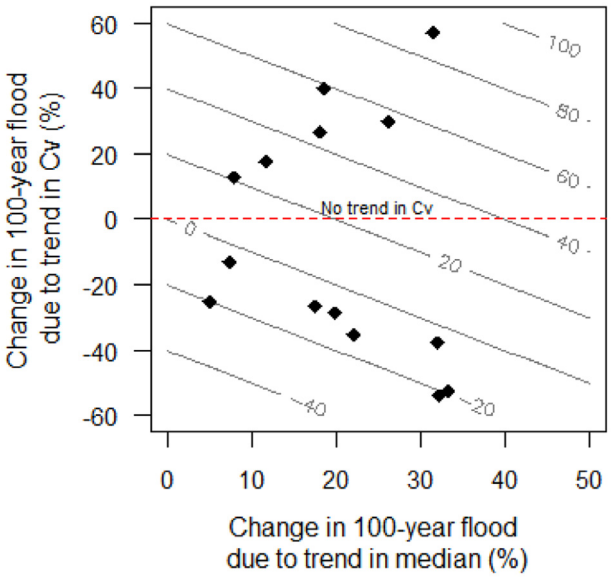

Fig. 6. Percent changes in the 100-year flood due to trends in the median and Cv at stations with (i) increasing median trends ($p < 0.05$) and (ii) either decreasing or increasing Cv trends ($p < 0.05$). Contours indicate the overall percent change in the 100-year flood relative to S-LN2 (stationary) 100-year flood estimate.

and Cv trends, $Q_{100yr}(\mu_{y|\omega},\sigma_{y|w})$ and the one only considering increases in the median $Q_{100yr}(\mu_{y|\omega})$:

$$\frac{Q_{100yr}(\mu_{y|\omega},\sigma_{y|w}) - Q_{100yr}(\mu_{y|\omega})}{Q_{100yr}} \tag{18}$$

We normalized the differences in $Q_{100yr}(\mu_{y|\omega},\sigma_{y|w})$ and $Q_{100yr}(\mu_{y|\omega})$ by Q_{100yr} to compare changes in 100-year flood estimates due to trends in the median and Cv, respectively. For example, an increasing median may lead to a 100-year flood estimate 50% greater than its stationary counterpart. However, the 100-year flood may not change at all if a decreasing Cv trend fully offsets the effects of an increasing median trend on the 100-year flood. In this case, (18) yields a value of -50%. Fig. 6 plots values of (17) and (18) for each of the 14 stations exhibiting significant increasing or decreasing Cv trends (see Table 2) using estimates for the most current year on record.

Fig. 6 illustrates the importance of accounting for both trends in the median and Cv when adjusting 100-year floods to reflect current basin conditions. The contours indicate the overall percent change in the 100-year flood relative to a S-LN2 (stationary) 100-year flood estimate. Stations with significant decreasing Cv trends register much lower 100-year flood estimates whereas stations with significant increasing Cv trends register much higher estimates. Overall, 100-year flood estimates considering both increasing trends in the median and Cv can exceed estimates assuming stationarity by more than 80%. Such changes are substantially larger than ones resulting from changes in the median alone.

Decreasing Cv trends can dramatically reduce design flood estimates adjusted for changes in central tendency. Even though our Monte Carlo simulations show that HET-NS-LN2 overestimates the 100-year flood, many stations in Fig. 6 lie below the 0% contour indicating no overall change in the 100-year flood when HET-NS-LN2 is used in lieu of S-LN2. In other words, at these stations, decreasing Cv trends lower 100-year flood estimates more than increasing median trends raise them. Again, there are two major statistical reasons for this tendency. First, the LN2 distribution is unable to consider asymmetrical changes to the variance of log-transformed flows. Second, when the conditional LN2 distribution is suitable for sites with increasing trends in the median and decreasing trends in the Cv, the stationary LN2 distribution is negatively skewed (see Appendix C). This negative skewness causes the 100-year flood to be overestimated. In fact, all eight stations with significant increasing median and decreasing Cv trends had negatively skewed samples (−0.32 to −0.94) when stationarity was assumed. While the null hypothesis of a stationary LN2 distribution could only be rejected at less than 13% of all 135 stations with well-behaved residuals, it was rejected at four out of eight stations with significant increasing median and decreasing Cv trends.

Finally, while we did not test the regional significance of trends, we examined spatial patterns qualitatively (see Fig. 5). Some previously reported regional change patterns are evident but, overall, they are not overwhelmingly strong, reflecting the relatively fragmented nature of flood nonstationarity in the conterminous US (Archfield et al., 2016). In some cases, strong urbanization impacts counter observed regional trends. For instance, at Glen Cove Creek at Glen Cove, New York (Gage ID = 01302500) the Cv decreases despite the extreme precipitation increase in the northeastern US (Huang et al., 2017).

Yet, a few known regional-scale climate-driven trends do appear in Fig. 1. Three decreasing Cv trends at north-central stations align with observed increases in the frequency but not the magnitude of floods there (Hirsch and Archfield, 2015; Mallakpour and Villarini, 2015), although this decrease is not observed at any of the nearby Chicago metropolitan area sites. Four of the six stations with increasing trends in the Cv are scattered throughout the northeastern United States. However, while this region underwent an increase in the 99th percentile daily precipitation in 1996 (Huang et al., 2017), the main increase in annual floods stems from an North Atlantic Oscillation-induced step change in 1970 (Armstrong et al., 2014). For instance, the Boston metropolitan area only has one station with an increasing Cv trend. The geographic dispersion of the four sites with increasing Cv trends in the eastern United States suggests that local hydrologic responses to urban development may contribute to these trends, especially since some are near stations with insignificant Cv decreases. (On the other hand, Seattle has several urbanizing sites with near-significant Cv increases near one site with a significant Cv increase.)

5. Discussion

This discussion begins by critically evaluating the models examined in this study before contemplating the incorporation of our method in flood management decision-making.

5.1. Model performance and recommendations

Our modeling framework enables evaluations of assumed trajectories of gradual change in flooding in response to increases in TIA. Here, our first-stage regression model assumes an exponential relationship between TIA and the AMS, which is mathematically equivalent to a linear relation between TIA and the logarithms of AMS. This functional form has nicely modeled changes in the median for AMS in numerous urbanizing environments (Vogel et al., 2011; Over et al., 2016), and suggests that the magnification of flooding accelerates as basins become more urbanized. However, changes in the logs of AMS may not be linearly related to changes in different indicators of urbanization, such as impervious cover. Moreover, recent stormwater regulations may temper urbanization-induced increases (Ntelekos, 2010; Zhou et al., 2017). This suggests that a logarithmic change trajectory may be more appropriate for basins with linear increases in impervious cover. Given that ladders-of-powers transformations enable many smooth monotonic trajectories of change to be modeled with regression, hypothesized functional forms reflecting varying trajectories of TIA and other indicators of hydrologic impacts of urbanization can be evaluated with our modeling framework. Since improperly specifying the functional form of the first-stage model can bias residual estimates and, in turn, affect second-stage models showing variability trends (Robinson and Birch, 2000), we examined alternative functional forms. However, we obtained a similar

set of basins with significant Cv trends with these alternative models for basins whose medians increased significantly (see Appendix F).

Other methods for modeling variability change trajectories also merit future attention. Notably, Yu and Stedinger (2018) examine the following model that assumes the log-space error variance changes exponentially in response to a linear change in a covariate ω:

$$\sigma^2_{\varepsilon|\omega} = \sigma^2_{\varepsilon|0} \exp\left(\beta_2 \omega\right) \tag{19}$$

After log-transforming this model, they use nonlinear least-absolute-value regression to estimate β_2. While not an OLS procedure, this relatively parsimonious method has numerous advantages, including that it prevents the variance from being negative (though ours did not yield negative values). Moreover, Aitkin (1987) demonstrated that IWLS-GLM can yield maximum likelihood estimates of this model's standard errors. Yet, while attractive for estimating change trajectories, log-transforming the squared residuals from the first-stage model is less likely to produce normally distributed residuals than HET-NS-LN2 (see Appendix B). This requires more complicated procedures for making inferences about Cv trends. Further, it remains unknown whether this change trajectory models observed changes in the Cv with more fidelity than HET-NS-LN2. It would be preferable to compare these two methods in a more expansive robustness study that also examines implications of mis-specifying variance change trajectories. In addition, regression models with binary indicator variables would enable the incorporation of abrupt changes in urban basins, such as flood-control reservoir construction (Over et al., 2016) or build-out (maximum permitted growth) dates.

Numerous other aspects of residual modeling also merit further investigation. First, comparing estimates from HET-NS-LN2 to ones that model trends in the first two conditional moments separately would illuminate the value of coupled models of conditional moments. Additional comparisons with other residual transformations (e.g. Efron, 1982) are also warranted. Last, we should examine the benefits of using studentized residuals to alleviate the effects of leverage from extreme observations near the ends of AMS on residuals (Robinson and Birch, 2000; Manning and Muhally, 2001).

5.2. Toward improved urban flood management

We introduce a NSFFA approach for estimating design floods that reflect current conditions in urbanizing basins, including changes in both the central tendency and the relative variability of AMS. We have only reported trends significant using a 5% significance level; this standard approach may neglect less pronounced trends that could modify the 100-year flood estimates substantially, especially when those trends are in the Cv. More research is needed to develop risk-based planning tools that consider both over- and under-design probabilities associated with type I and II errors from both median and Cv trends. (See Rosner et al. (2014) and Prosdocimi et al. (2014) for some initial efforts with trends in central tendency.) In practice, applications of our two-stage approach should examine the sensitivity of trend assessments to the start and end dates of AMS (Burn and Whitfield, 2018) and large historical floods outside of gauging periods (e.g. Cohn et al., 1997). Finally, if future design flood quantiles of interest are sought, we strongly recommend reporting prediction intervals for any extrapolated estimates, which tend to widen quickly with time and document our (in)ability to predict the future.

The extent to which Cv trends can modify 100-year flood estimates motivates future studies that attribute such trends to physical phenomena associated with urbanization and disentangle them from concurrent climatic fluctuations. Oudin et al. (2018) employed a "model residual" approach that assessed urbanization impacts to high flows (Q95) by calibrating a rainfall-runoff model during a pre-urbanization period and then running it during a post-urbanization period. Differences between observed and simulated flows during the post-urbanization period were attributed to urbanization, although the possible systematic underestimation of high flows from their continuous simulation model (see Farmer and Vogel, 2016) may confound their conclusions. Yet, if continuous simulation models can be improved or bias-corrected, statistical analyses of the results of factorial design experiments using mechanistic models (e.g. Jato-Espino et al., 2017) could also elucidate specific drivers of urban flood variability, such as effective impervious area (Ebrahimian et al., 2016), stormwater detention, and road construction.

6. Conclusions

When responding to increasing trends in AMS, decision-makers need nonstationary flood frequency analysis (NSFFA) methods that are easy to implement and address stakeholder needs. Previous studies (e.g. Vogel et al., 2011; Prosdocimi et al., 2014) have demonstrated the numerous benefits of ordinary least squares (OLS) regression for adjusting design floods by solely accounting for changes in the mean of AMS natural logarithms. To extend these efforts, we introduced a two-stage OLS regression model that accounts for changes in the Cv of AMS. We applied this approach to 135 stations in urbanizing basins with (i) drainage areas of at least 5 km^2, (ii) TIA exceeding 10% at one point in their record, (iii) record lengths of 30 years or longer without any extensive intermittency in gauging and (iv) conditional median models with normally distributed and temporally uncorrelated residuals. Of the 67 stations exhibiting significant (95% level) increases in their medians, 21% (14/135) had concurrent Cv trends (see Table 2). This suggests that HOM-NS-LN2, which assesses trends strictly in medians, often ends up being a viable first-order approach for characterizing observed changes in design flood quantiles in urbanizing basins whose AMS exhibit nonstationary behavior and normal residuals (Vogel et al., 2011). However, we document the importance of incorporating Cv trends into 100-year flood estimates, which have societal ramifications ranging from bridge design to property insurance.

Finally, challenges modeling the asymmetrical changes in variability in urbanizing basins and comparing stationary and nonstationary versions of theoretical distributions motivate the development of other models for basins with decreasing Cv trends. This motivates the use of three-parameter probability distributions (e.g. LP3) where changes in skewness can partially compensate for changes in variability. Indeed, this work combined with Serago and Vogel (2018) provides an OLS regression-based conditional moments framework for determining the conditional skewness of AMS in response to changes in the mean and variance of log-transformed flows. To reflect the tendency for urbanization to magnify larger annual floods much less than smaller ones, statistical approaches that enable a fixed upper bound, such as the GEV Type III distribution and quantile regression, should also be investigated. Future work should also evaluate our two-stage approach for partial duration series (peaks-over-threshold), which has recently demonstrated a stronger association with urbanization than AMS (Prosdocimi et al., 2015), or even complete daily flow time series (Serinaldi et al., 2018). Finally, we encourage applications of this modeling framework that assess other hydroclimatic extremes.

Declaration of Competing Interest

The authors declare that they have no known competing financial interests or personal relationships that could have appeared to influence the work reported in this paper.

Acknowledgements and data

The authors are indebted to the U.S. Army Corps of Engineers (USACE), Institute for Water Resources (IWR) for their encouragement and support of this research. The second author was supported by an appointment to the U.S. Army Corps of Engineers (USACE) Research Participation Program administered by the Oak Ridge Institute for Science and Education (ORISE) through an interagency agreement between

the U.S. Department of Energy (DOE) and the U.S. Army Corps of Engineers (USACE). ORISE funding was managed by ORAU (DE-AC05-06OR23100). All opinions expressed in this paper are the authors' and do not necessarily reflect the policies and views of USACE, IWR, DOE, or ORAU/ORISE. Two National Science Foundation grants enabled Tufts University (Water Diplomacy: NSF OIA-0966093) and the University of Vermont (BREE: NSF OIA-1556770) to provide in-kind support. The authors are also grateful for earlier reviews and discussions with Annalise Blum, Jake Serago, Nancy Barth, and Karen Ryberg.

All data used are publicly available. The observed annual maximum series (instantaneous peak flow) data are available from the National Water Information System at http://waterdata.usgs.gov/nwis. Total impervious area (TIA) data were derived from historical housing density data used in the US Environmental Protection Agency's Integrated Climate and Land-Use Scenarios (ICLUS) project (https://www.epa.gov/iclus). Other watershed characteristics were obtained from the GAGES II dataset (Falcone, 2011). Models used in this study are available from the authors upon request.

Supplementary materials

Supplementary material associated with this article can be found, in the online version, at doi:10.1016/j.advwatres.2019.103484.

References

Ahn, K.-H., Palmer, R.N., 2015. Trend and variability in observed hydrological extremes in the United States. J. Hydrol. Eng. 10.1061/(ASCE)HE.1943-5584.0001286.

Aissaoui-Fqayeh, I., El-Adlouni, S., Ouarda, T.B.M.J., St.-Hilaire, A., 2009. Développement du modèle log-normal nonstationnaire et comparaison avec le modèle GEV nonstationnaire. Hydrol. Sci. J. 54 (6), 1141–1156.

Aissaoui-Fqayeh, I., El-Adlouni, S., Ouarda, T.B.M.J., St.-Hilaire, A., 2006. Développement de l'estimateur GLM-ML pour le modèle log-normal nonstationnaire et application à des précipitations extremes. *Research report R-860*[Available at http://espace.inrs.ca/583/1/R000860.pdf].

Aitkin, M., 1987. Modelling variance heterogeneity in normal regression using GLIM. Appl. Stat. – J. Roy. St. C 36, 332–339.

Allaire, M.C., Vogel, R.M., Kroll, C.N., 2015. **The hydromorphology of an urbanizing watershed using multivariate elasticity**. Advances in Water Resources 86, 147–154. https://doi.org/10.1016/j.advwatres.2015.09.022.

Anscombe, F.J., 1953. Contribution to the discussion of H. Hotelling's paper. J. Roy. Stat. Soc. B 15, 165–173.

Archfield, S.A., Hirsch, R.M., Viglione, A., Blöschl, G., 2016. Fragmented patterns of flood change across the United States. Geophys. Res. Lett. https://doi.org/10.1002/2016GL070590.

Armstrong, W. (2014), M.J. Collins, N.A. Snyder (2014), Hydroclimatic flood trends in the northeastern United States with linkages to large-scale atmospheric circulation patterns.

Association of State Floodplain Managers (ASFPM) (2016), *Meeting the challenge of change: implementing the federal flood risk management standard and climate-informed science approach*. [Available at http://www.asfpmfoundation.org/ace-images/forum/Meeting_the_Challenge_of_Change.pdf].

Ball, J., 2016. In: Babister, M., Nathan, R., Weeks, W., Weinmann, E., Retallick, M., Testoni, I. (Eds.), Australian Rainfall and Runoff: a Guide to Flood Estimation. Commonwealth of Australia. [Available at www.arr.org.au/arr-guideline/].

Bates, B.C., Chandler, R.E., Bowman, A.W., 2012. Trend estimation and change point detection in individual climatic series using flexible regression methods. J. Geophys. Res. 117, D16016. https://doi.org/10.1029/2011JD017077.

Beam, J.D., Braunscheidel, J.J., 1998. Rouge River Assessment. State of Michigan Department of Natural Resources. Fisheries Division Special Report 22. [Available at http://www.michigandnr.com/PUBLICATIONS/PDFS/ifr/ifrlibra/Special/Reports/sr22.pdf].

Beard, L.R. (1974), *Flood Flow Frequency Techniques*. Center for Research in Water Resources, Univ. of Texas at Austin. [Available at http://water.usgs.gov/osw/bulletin17b/Beard_FFFT_1974.pdf]

Beighley, R.E., Moglen, G.E., 2003. Adjusting measured peak discharge from an urbanizing watershed to reflect a stationary land use signal. Water Resour. Res. 39 (4), 1093–1103. https://doi.org/10.1029/2002WR001846.

Berton, R., Driscoll, C.T., Adamowski, J.F., 2017. The near-term prediction of drought and flooding conditions in the northeastern United States based on extreme phases of AMO and NAO. J. Hydrol. 553, 130–141.

Braud, I., Breil, P., Thollet, F., Lagouy, M., Branger, F., Jacqueminet, C., Kermadi, S., Michel, K., 2013. Evidence of the impact of urbanization on the hydrological regime of a medium-sized periurban catchment in France. J. Hydrol. 485, 5–23.

Breusch, T.S., Pagan, A.R., 1979. A simple test for heteroscedasticity and random coefficient variation. Econometrica 47 (5).

Burn, D.H., Whitfield, P.H., 2018. Changes in flood events inferred from centennial length records. Adv. Water Resour. 121, 333–349.

Carroll, R.J., Ruppert, D., 1988. Transformation and Weighting in Regression. Chapman & Hall.

Chandler, R.E., Wheater, H.S., 2002. Analysis of rainfall variability using generalized linear models: a case study from the west of Ireland. Water Resour. Res. 38 (10), 1192. https://doi.org/10.1029/2001WR000906.

Chao Lim, T., 2016. Predictors of urban variable source area: a cross-sectional analysis of urbanized catchments in the United States. Hydrol. Proc. 30, 4799–4814. https://doi.org/10.1002/hyp.10943.

Clarke, R.T., 2002. Estimating time trends in Gumbel-distributed data by means of generalized linear models. Water Resour. Res. 38 (7). https://doi.org/10.1029/2001WR000917.

Clarke, R.T., 2001. Separation of year and site effects by generalized linear models in regionalization of annual floods. Water Resour. Res. 37 (4), 979–986.

Cohn, T.A., Lins, H.F., 2005. Nature's style: naturally trendy. Geophys. Res. Let. 32, L23402. https://doi.org/10.1029/2005GL024476.

Cohn, T.A., Lane, W.L., Baier, W.G., 1997. An algorithm for computing moments-based flood quantile estimates when historical flood information is available. Water Resour. Res. 33 (9), 2089–2096.

Condon, L.E., Gangopadhyay, S., Pruitt, T., 2015. Climate change and non-stationary flood risk for the upper Truckee River basin. Hydrol. Earth Syst. Sci. 19, 159–175.

Cunderlik, J., Burn, D., 2003. Non-stationary pooled flood frequency analysis. J. Hydrol. 276, 210–223.

Davidian, M., Haaland, P.D., 1990. Regression and calibration with non-constant error variance. Chemometr. Intell. Lab. 9, 231–248.

Davidian, M., Carroll, R.J., 1987. Variance function estimation. J. Am. Stat. Assoc. 82 (400), 1079–1091.

Debbage, N., Shepherd, J.M., 2018. The influence of urban development patterns on streamflow characteristics in the Charlanta megaregion. Water Resour. Res. 54. https://doi.org/10.1029/3017WR021594.

Delgado, J.M., Merz, B., Apel, H., 2014. Projecting flood hazard under climate change: an alternative approach to model chains. Nat. Hazards Earth Syst. Sci. 14, 1579–1589.

Delgado, J.M., Apel, H., Merz, B., 2010. Flood trends and variability in the Mekong River. Hydrol. Earth Syst. Sc. 14, 407–418.

Diem, J.E., Hill, T.C., Milligan, R.A., 2018. Diverse multi-decadal changes in streamflow within a rapidly urbanizing region. J. Hydrol. 556, 61–71.

Douglas, E.M., Vogel, R.M., Kroll, C.N., 2000. Trends in floods and low flows in the United States: impact of spatial correlation. J. Hydrol. 240, 90–105.

Ebrahimian, A., Gulliver, J.S., Wilson, B.N., 2016. Effective impervious area for runoff in urban watersheds. Hydrol Process 30, 3717–3729.

Efron, B, 1982. Transformation theory: how normal is a family of distributions? Ann. Stat. 10 (2), 323–339 JSTOR, www.jstor.org/stable/2240670.

England Jr., J.F., Cohn, T.A., Faber, B.A., Stedinger, J.R., Thomas Jr., W.O., Veilleux, A.G., Kiang, J.E., Mason Jr., R.R., 2018. Guidelines for Determining Flood Flow Frequency – Bulletin 17C. U.S. Geological Techniques and Methods. https://doi.org/10.3133/tm4B5. book 4, chap. B5[Available at https://pubs.usgs.gov/tm/04/b05/tm4b5.pdf.].

Falcone, J.A., 2011. Geospatial Attributes of Gages for Evaluating Streamflow (GAGES II) - Summary report [Available at https://water.usgs.gov/GIS/metadata/usgswrd/XML/gagesII_Sept2011.xml] .

Farmer, W.H., Vogel, R.M., 2016. On the deterministic and stochastic use of hydrologic models. Water Resour. Res. 52. https://doi.org/10.1002/2016WR019129.

Fathian, F., Fakheri-Fard, A., Ouarda, T.B.M.J., Dinpashoh, Y., Mousavi Nadoushani, S.S., 2019. Multiple streamflow time series modeling using VAR-MGARCH approach. Stoch. Envir. Res. Risk Assess. https://doi.org/10.1007/s00477-019-01651-9.

Federal Emergency Management Agency(FEMA) and Department of Homeland Security (DHS) (2018), Updates to floodplain management and protection of wetlands regulations to implement executive order 13690 and the federal flood risk management standard. Accessed at https://www.federalregister.gov/documents/2018/03/06/2018-04495/updates-to-floodplain-management-and-protection-of-wetlands-regulations-to-implement-executive-order on September 4, 2019.

Ferreira, C.S.S., Walsh, R.P.D., Steenhuis, T.S., Shakesby, R.A., Nunes, J.P.N., Coelho, C.O.A., Ferreira, A.J.D., 2015. Spatiotemporal variability of hydrologic soil properties and the implications for overland flow and land management in a peri-urban Mediterranean catchment. J. Hydrol. 525, 249–263.

Gilroy, K.L., McCuen, R.H., 2012. A nonstationary flood frequency analysis method to adjust for future climate and urbanization. J. Hydrol. 414-415, 40–48.

Gregory, J.H., Dukes, M.D., Jones, P.H., Miller, G.L., 2006. Effect of urban soil compaction on infiltration rate. J. Soil Water Conserv. 61 (3), 117–124.

Harvey, A.C., 1976. Estimating regression models with multiplicative heteroscedasticity. Econometrica 44, 461–465.

Hecht, J.S., 2017. Making Multi-Stakeholder Water Resources Decisions with Limited Streamflow Information. Department of Civil and Environmental Engineering, Tufts University.

Hirsch, R.M., 1977. The interaction of channel size and flood discharges for basins undergoing urbanization. Intl. Assoc. Sci. Hydrol. Pub. 123, 83–92.

Hirsch, R.M., Archfield, S.A., 2015. Flood trends: Not higher but more often. Nat. Clim. Change 5, 198–199.

Hodgkins, G.A., Whitfield, P.A., Burn, D.H., Hannaford, J., Renard, B., Stahl, K., Fleig, A., Madsen, H., Medeiro, L., Korhonen, J., Murphy, C., Wilson, D., 2017. Climate-driven variability in the occurrence of major floods across North America and Europe. J. Hydrol. https://doi.org/10.1016/j.jhydrol.2017.07.027.

Hollis, G.E., 1975. The effect of urbanization on floods of different recurrence interval. Water Resour. Res. 11 (3), 431–435.

Hopkins, K.G., Morse, N.B., Bain, D.J., Bettez, N.D., Grimm, N.B., Morse, J.L., Palta, M.M., Shuster, W.D., Bratt, A.R., Suchy, A.K., 2015. Assessment of regional variation in streamflow responses to urbanization and the persistence of physiography. Environ. Sci. Tech. 49, 2724–2732.

Huang, H., Winter, J.M., Osterberg, E.C., Horton, R.M., Beckage, B., 2017. Total and extreme precipitation changes over the Northeastern United States. J. Hydrometeor. 18, 1783–1798.

Jain, S., Lall, U., 2000. Magnitude and timing of annual maximum floods: trends and large-scale climate associations for the Blacksmith Fork River, Utah. Water Resour. Res. 36 (12), 3641–3651.

Jato-Espino, D., Sillanpää, N., Charlesworth, S.M, Rodríguez-Hernández, J., 2017. A simulation-optimization methodology to model urban catchments under non-stationary extreme rainfall events. Environ. Modell. Softw. https://doi.org/10.1016/j.envsoft.2017.05.008.

Jato-Espino, D., Sillanpää, N., Andrés-Doménech, I., Rodríguez-Hernández, J., 2018. Flood risk assessment in urban catchments using multiple regression analysis. J. Water Resour. Plann. Manage. https://doi.org/10.1061/ASCEWR.1943-5452.0000874.

Katz, R., Brown, B., 1992. Extreme events in a changing climate: variability is more important than averages. Clim. Change 21, 289–302.

Kelbore, Z.G., 2012. An analysis of the impacts of climate change on crop yield and yield variability in Ethiopia. Munich Personal RePEc Archive Paper 49466. Available at http://mpra.ub.uni-muenchen.de/49466] .

Khaliq, M.N., Ouarda, T.B.M.J., Ondo, J.-C., Gachon, P., Bobée, B., 2006. Frequency analysis of a sequence of dependent and/or non-stationary hydro-meteorological observations: a review. J. Hydrol. 329, 534–552.

Kigobe, M., McIntyre, N., Wheater, H., Chandler, R., 2011. Multi-site stochastic modelling of daily rainfall in Uganda. Hydrol. Sci. J. 56 (1), 17–33.

Kjeldsen, T.R., 2010. Modelling the impact of urbanization on flood frequency relationships in **the UK**. Hydrol. Res. 41 (5), 391–405. https://doi.org/10.2166/nh.2010.056.

Kjeldsen, T.R., 2009. An exploratory analysis of error components in hydrological regression modeling. Water Resour. Res. 45, W02407. https://doi.org/10.1029/2007WR006283.

Kjeldsen, T.R., D.A. Jones, and A.C. Bayliss (2008), Improving the FEH (Flood Estimation Handbook) statistical procedures for flood frequency estimation. Science Report SC05050. Environment Agency and Department for Environment, Food and Rural Affairs. [Available at https://www.gov.uk/government/publications/improving-the-flood-estimation-handbook-feh-statistical-procedures-for-flood-frequency-estimation]

Kokonnen, T.V., Grimmond, C.S.B., Christen, A., Oke, T.R., Järvi, L., 2018. Changes to the water balance over a century of development in two neighborhoods: Vancouver, Canada. Water Resour. Res. https://doi.org/10.1029/2017WR022445.

Kuczera, G., 1982. Robust flood frequency models. Water Resour. Res. 18 (2), 315–324.

Kundzewicz, Z.Wand many others, 2014. Flood risk and climate change: global and regional perspectives. Hydrol. Sci. J. 59 (1), 1–28. https://doi.org/10.1080/02626667.2013.857411.

Kwon, H.-H., Brown, C., Lall, U., 2008. Climate informed flood frequency analysis and prediction in Montana using hierarchical Bayesian modeling. Geophys. Res. Let. 35.

Latraverse, M., Rasmussen, P.F., Bobée, B., 2002. Regional estimation of flood quantiles: parametric versus nonparametric regression models. Water Resour. Res. 38 (6), 1095. https://doi.org/10.1029/2001WR000677.

Lee, J.G., Heaney, J.P., 2003. Estimation of urban imperviousness and its impacts on storm water systems. J. Water Resour. Plann. Manage. 129 (5), 419–426.

Leopold, L.B., 1968. Hydrology for Urban Planning – a Guidebook on the Hydrologic Effects of Urban Land Use, 556. U.S. Geological Survey Tech. Rep, Washington, D.C.

Lim, T.C., 2016. Predictors of urban variable source area: a cross-section analysis of urbanized catchments in the United States. Hydrol. Process. 30 (25), 4799–4814.

Locatelli, L., Mark, O., Mikkelsen, P.S., Arnbjerg-Nielsen, K., Deletic, A., Roldin, M., Binning, P.J., 2017. Hydrologic impact of urbanization with extensive stormwater infiltration. J. Hydrol. 544, 524–537.

Long, J.S., Ervin, L.H., 2000. Using heteroscedasticity consistent standard errors in the linear regression model. Am. Stat. 54 (3), 217–223.

López, J., Francés, F., 2013. Non-stationary flood frequency analysis in continental Spanish rivers, using climate and reservoir indices as external covariates. Hydrol. Earth Syst. Sc. 17, 3189–3203.

Luke, A., Vrugt, J.A., AghaKouchak, A., Matthew, R., Sanders, B.F., 2016. Predicting nonstationary flood frequencies: evidence supports an updated stationarity thesis in the United States. Water Resour. Res. 53. https://doi.org/10.1002/2016WR019676.

Madsen, H., Lawrence, D., Lang, M., Martinkova, M., Kjeldsen, T.R., 2013. A review of applied methods in Europe for flood-frequency analysis in a changing environment. COST Action ES0901: Flood Frequency Estimation Methods And Environmental Change. Centre for Ecology and Hydrology. [Available at http://nora.nerc.ac.uk/id/eprint/501751/].

Mallakpour, I., Villarini, G., 2015. The changing nature of flooding across the central United States. Nat. Clim. Change 5, 250–254.

Manning, W.G., Mullahy, J., 2001. Estimating log models: to transform or not to transform? J. Health Econ. 20, 461–494.

Matalas, N.C., Sankarasubramanian, A., 2003. Effect of persistence on trend detection via regression. Water Resour. Res. 39 (12), 1342. https://doi.org/10.1029/2003WR002292.

McCabe, G.J., Wolock, D.M., 2002. A step increase in streamflow in the conterminous United States. Geophys. Res. Let. 29 (24), 2185. https://doi.org/10.1029/2002GLO15999.

McCuen, R.H., 2003. Modeling Hydrologic Change: Statistical Methods. Lewis Publishers, Boca Raton, Fla., p. 433.

Mejía, A.I., Moglen, G.E., 2010. Impact of the spatial distribution of imperviousness on the hydrologic response of an urbanizing basin. Hydrol. Process. 24 (23), 3359–3373.

Miller, J.D., Kim, H., Kjeldsen, T.R., Packman, J., Grebby, S., Dearden, R., 2014. Assessing the impact of urbanization on storm runoff in a peri-urban catchment using historical change in impervious cover. J. Hydrol. 515, 59–70.

Minto, C., Myers, R.A., Blanchard, W., 2008. Survival variability and population density in fish populations. Nature 20, 452 (7185), 344–347.

Montanari, A., Koutsoyiannis, D., 2014. Modeling and mitigating natural hazards: stationarity is immortal!. Water Resour. Res. 50, 9748–9756. https://doi.org/10.1002/2014WR016092.

Mosteller, F., Tukey, J.W., 1977. Data Analysis and Regression. Addison-Wesley Publishers, Menlo Park, CA, p. 588.

Najibi, N., Devineni, N., 2018. Recent trends in the frequency and duration of global floods. Earth Syst. Dynam. 9, 757–783.

Ntelekos, A.A., Oppenheimer, M., Smith, J.A., Miller, A.J., 2010. Urbanization, climate change and flood policy in the United States. Climatic Change 103, 597–616.

O'Brien, N.L., Burn, D.H., 2014. A nonstationary index-flood technique for estimating extreme quantiles for annual maximum streamflow. J. Hydrol. 519B, 2040–2048. https://doi.org/10.1016/j.jhydrol.2014.09.041.

Ogden, F.L., Pradhan, N.R., Downer, C.W., Zahner, J.A., 2011. Relative importance of impervious area, drainage density, width function, and subsurface storm drainage on flood runoff from an urbanized catchment. Water Resour. Res. 47, W12503. https://doi.org/10.1029/2011WR010550.

Oudin, L., Salavati, B., Furusho-Percot, C., Ribstein, P., Saadi, M., 2018. Hydrological impacts of urbanization at the catchment scale. J. Hydrol. https://doi.org/10.1016/j.jhydrol.2018.02.064.

Over, T.M., Saito, R.J., Soong, D.T., 2016. Adjusting Annual Maximum Peak Discharges at Selected Stations in Northeastern Illinois for Changes in Land-Use Conditions. *U.S. Geological Survey Scientific Investigations Report 2016-5049*[Available at http://pubs.usgs.gov/sir/2016/5049/sir20165049.pdf] .

Pallard, B., Castellarin, A., Montanari, A., 2009. A look at the links between drainage density and flood statistics. Hydrol. Earth Syst. Sci. 13, 1019–1029.

Park, R.E., 1966. Estimation with heteroscedastic error terms. Econometrica 34 (4), 888.

Paulson, R.W., Chase, E.B., Roberts, R.S., Moody, D.W., 1991. National Water Summary 1988-89: Hydrologic Events and Floods and Droughts 2375. *U.S. Geological Survey Water Supply Paper*[Available at https://pubs.er.usgs.gov/publication/wsp2375] .

Prosdocimi, I., Kjeldsen, T.R., Miller, J.D., 2015. **Detection and attribution of urbanization effect on flood extremes using nonstationary flood-frequency models**. Water Resources Research 51 (6), 4244–4262. https://doi.org/10.1002/2015WR017065.

Prosdocimi, I., Kjeldsen, T.R., Svensson, C., 2014. Non-stationarity in annual and seasonal series of peak flow and precipitation in the UK. Nat. Hazards Earth Syst. Sci. 14, 1125–1144.

R Core Team, 2019. R: A Language and Environment for Statistical Computing. Foundation for Statistical Computing, Vienna: R [Available at https://www.R-project.org/] .

Read, L.K., Vogel, R.M., 2015. Reliability, return periods, and risk under nonstationarity. Water Resour. Res. 51. https://doi.org/10.1002/2015WR017089.

Redfern, T.W., Macdonald, N., Kjeldsen, T.R., Miller, J.D., Reynard, N., 2016. Current understanding of hydrological processes on common urban surfaces. Prog. Phys. Geog. 40 (5), 699–713.

Robinson, T.J., Birch, J.B., 2000. Model misspecification in parametric dual modeling. J. Stat. Comput. Sim. 66, 113–126.

Rosner, A., Vogel, R.M., Kirshen, P.H., 2014. A risk-based approach to flood management decisions in a nonstationary world. Water Resour. Res. 50. https://doi.org/10.1002/2013WR014561.

Salas, J.D., Obeysekera, J., Vogel, R.M., 2018. Techniques for assessing water infrastructure for nonstationary extreme events: a review. Hydrol. Sci. J. https://doi.org/10.1080/02626667.2018.1426858.

Salavati, B., Oudin, L., Furusho, C., Ribstein, P., 2016. Modeling approaches to detect land-use changes: urbanization analyzed on a set of 43 US catchments. J. Hydrol. 537. https://doi.org/10.1016/j.jhydrol.2016.04.010.

Salvadore, E., Bronders, J., Batelaan, O., 2015. Hydrological modelling of urbanized catchments: a review and future directions. J. Hydrol. 529 (Part 1), 62–81.

Schueler, T.R., Fraley-McNeal, L., Cappiella, K., 2009. Is impervious cover still important? Review of recent research. J. Hydrol. Eng. 14 (4), 309–315 10.1 061/(ASCE) 1 084-0699(2009) 14:4(309).

Serago, J.M., Vogel, R.M., 2018. Parsimonious nonstationary flood frequency analysis. Adv. Water Resour. 112, 1–16.

Serinaldi, F., Kilsby, C.G., Lombardo, F., 2018. Untenable nonstationarity: an assessment of the fitness for purpose of trend tests in hydrology. Adv. Water Resour. 111, 132–155.

Serinaldi, F., Kilsby, C.G., 2015. Stationarity is undead: Uncertainty dominates the distribution of extremes. Adv. Water Resour. 77, 17–36.

Slater, L., Villarini, G., 2016. On the impacts of gaps on trend detection in extreme streamflow time series. Int. J. Cliimatol. https://doi.org/10.1002/joc.4954.

Smith, B.K., Smith, J.A., Baeck, M.L., Villarini, G., Wright, D.B., 2013. Spectrum of storm event hydrologic response in urban watersheds. Water Resour. Res. 49, 2649–2663. https://doi.org/10.1002/wrcr.20223.

Smyth, G.K., Huele, A.F., Verbyla, A.P., 2001. Exact and approximate REML for heteroscedastic regression. Stat. Model. 1, 161–175.

Spence, C.M., Brown, C.M., 2016. Nonstationary decision model for flood risk decision scaling. Water Resour. Res. 52, 8650–8667. 10.1002/2016WR018981.

Stedinger, J.R., 2016. Flood frequency analysis. Chapter 76. In: Singh, V.P. (Ed.), Handbook of Applied Hydrology. McGraw Hill Book Co.

Stedinger, J.R., 1983. Design events with specified flood risk. Water Resour. Res. 19 (2), 511–522.

Stedinger, J.R., 1980. Fitting log normal distributions to hydrologic data. Water Resour. Res. 16 (3), 481–490.

Stedinger, J.R., Tasker, G.D., 1985, Regional hydrologic analysis: 1. ordinary, weighted and generalized least squares compared, 21(9), 1421-1432.

Stedinger, J.R., Griffis, V.W., 2011. Getting From Here to Where? Flood Frequency Analysis and Climate. J. Am. Water Resour. Assoc. 47 (3), 506–513. https://doi.org/10.1111/j.1752-1688.2011.00545.x.

Stedinger, J., Vogel, R.M., Foufoula-Georgiou, E., 1993. Chapter 18 in handbook of hydrology. In: Maidment, DR (Ed.), Frequency Analysis of Extreme Events. McGraw-Hill.

Strupczewski, W.G., Singh, V.P., Mitosek, H.T., 2001. Non-stationary approach to at-site flood frequency modeling III. Flood analysis of Polish rivers. J. Hydrol. 248, 152–167.

Sun, R., Yuan, H., Liu, X., 2017. Effect of heteroscedasticity treatment in residual error models on model calibration and prediction uncertainty estimation. J. Hydrol. https://doi.org/10.1016/j.jhydrol.2017.09.041.

Theobald, D., 2005. Landscape patterns of exurban growth in the United States. Ecol. Soc. 10 (1), 32.

Trudeau, M.P., Richardson, M., 2016. Change in event-scale hydrologic response in two urbanizing watersheds of the Great Lakes-St Lawrence Basin 1969-2010. J. Hydrol. 523, 650–662.

U.S. Army Corps of Engineers, 1993. Hydrologic Frequency Analysis: EM 1110-2-1415 U.S. Army Corps of Engineers, Washington, D.C. Accessed at http://www.publications.usace.army.mil/portals/76/publications/engineermanuals/em_1110-21415.pdf on August 22, 2019.

Vandenberg-Rodes, A., Moftakhari, H.R., AghaKouchak, A., Shahbaba, B., Sanders, B.F., Matthew, R.A., 2016. Projecting nuisance flooding in a warming climate using generalized linear models and Gaussian processes. J. Geophys. Res. https://doi.org/10.1002/2016JC012084.

Villarini, G., Serinaldi, F., Smith, J.A., Krajewski, W., 2009a. On the stationarity of annual flood peaks in the continental United States during the 20th century. Wat. Resour. Res. 45. https://doi.org/10.1029/2008WR007645.

Villarini, G., Smith, J.A., 2010. Flood peak distributions for the eastern United States. Water Resour. Res. 46, W06504. https://doi.org/10.1029/2009WR008395.

Villarini, G., Smith, J.A., Serinaldi, F., Bales, J., Bates, P.D., Krajewski, W.F., 2009b. Flood frequency analysis for nonstationary annual peak records in an urban drainage basin. Adv. Water Resour. 32, 1255–1266.

Villarini, G., Taylor, S., Wobus, C., Vogel, R.M., Hecht, J.S., White, K., Baker, B., Gilroy, K., Olsen, J.R., Raff, D., 2018. Floods and Nonstationarity: A Review. CWTS 2018-01. U.S. Army Corps of Engineers, Washington, DC [Available at https://usace.contentdm.oclc.org/digital/collection/p266001coll1/id/6036/] .

Vogel, R.M., Yaindl, C., Walter, M., 2011. Non-stationarity: Flood magnification and recurrence reduction factors in the United States. J. Am. Wat. Res. Assoc. 47 (3), 464–474.

Vogel, R.M., Wilson, I., 1996. Probability distribution of annual maximum, mean, and minimum streamflow in the United States. J. Hydrol. Eng. 1 (2), 69–76.

Wang, W., van Gelder, P.H.A.J.M., Vrijling, J.K., Ma, J., 2005. Testing and modelling autoregressive conditional heteroscedasticity of streamflow processes. Nonlin. Proc. Geophys. 12, 55–66.

Weng, Q., 2012. Remote sensing of impervious surfaces in the urban area: requirements methods, and trends. Remote Sens. Environ. 117, 34–49.

Western, B., Bloome, D., 2009. Variance function regressions for studying inequality. Sociol. Methodol. 39 (1), 293–326.

Yang, G., Bowling, L., Cherkauer, K., Pijanowski, B., Niyogi, D., 2010. Hydroclimatic response of watersheds to urban intensity: an observational and modeling-based analysis for the White River Basin, Indiana. J. Hydrometeorol. 11, 122–138.

Yang, L., Smith, J.A., Baeck, M.L., Bou-Zeid, E., Jessup, S.M., Tian, F., Hu, H., 2014. Impact of urbanization on heavy convective precipitation under strong large-scale forcing: a case study over the Milwaukee-Lake Michigan region. J. Hydrometeor. 15, 261–278.

Yu, X., Stedinger, J.R., 2018. LP3 flood frequency analysis including climate change. In: World Environmental and Water Resources Congress. American Society of Civil Engineers, Reston, Va, pp. 459–467. Available at https://ascelibrary.org/doi/10.1061/9780784481400.043.

Zhang, Y., Cromley, R.G., Hanink, D.M., 2015. A spatial hedonic model application of variance function regression to residential property prices in Beijing. Lett. Spat. Resour. Sci. https://doi.org/10.1007/s12076-015-0142-6.

Zhang, W., Villarini, G., Vecchi, G.A., Smith, J.A., 2018. Urbanization exacerbated the rainfall and flooding caused by hurricane Harvey in Houston. Nature 563, 384–388.

Zheng, H., Yang, Y., Land, K.C., 2013. Heteroscedastic regression models for the systematic analysis of residual variances. Chapter 3. Handbook of Causal Analysis for Social Research, pp. 133–152.

Zhou, Z., Smith, J.A., Yang, J.A., L., Baeck, M.L., Chaney, M., ten Veldhuis, M.-C., Deng, H., Liu, S., 2017. The complexities of urban flood response: flood frequency analyses for the Charlotte metropolitan region. Water Resour. Res. https://doi.org/10.1002/2016WR019997.